TECHNICAL REPORT NO. 61

APRIL 1, 1954

AN ANALYSIS OF THE MESON COMPONENT OF COSMIC RAYS IN THE ATMOSPHERE

By

STANISLAW OLBERT

LABORATORY FOR NUCLEAR SCIENCE AND ENGINEERING

MASSACHUSETTS INSTITUTE OF TECHNOLOGY

Cambridge, Massachusetts

Technical Report No. 61

April 1, 1954

AN ANALYSIS OF THE MESON COMPONENT OF

COSMIC RAYS IN THE ATMOSPHERE*

By

Stanislaw Olbert

ABSTRACT

The meson component of cosmic rays in the atmosphere is investigated quantitatively with respect to its various fundamental characteristics. The analysis is based on a unidimensional equation for the vertical differential intensity of μ-mesons, studied originally by M. Sands. The following topics are discussed in detail:

(1) The a priori unknown range spectrum of μ-mesons at production, $G(R')$, is derived from Sands' equation with the aid of recent experimental data concerning the μ-meson intensity. These include the altitude and latitude dependence of μ-meson intensities as well as the momentum distribution of μ-mesons at sea level. It is shown that, for the residual ranges 100 g cm$^{-2} < R' < 6,000$ g cm^{-2}, the production spectrum may be represented by the following empirical formula:

$$G(R') = \frac{7.31 \times 10^{4}}{(a+R')^{3.58}} \qquad \left[g^{-2} cm^{2} sec^{-1} sterad^{-1} \right]$$

where a is a constant characteristic for a given geomagnetic latitude. The values of a vary from 646 g cm^{-2} at the geomagnetic equator to 513 g cm^{-2} at $60°$ geomagnetic latitude. The value of 520 g cm^{-2} at $50°$ geomagnetic latitude is considered as the most reliable, since at this latitude the experimental data are most complete. The production spectrum is compared with that derived by M. Sands on the basis of earlier, less accurate observational material.

(2) The effects of atmospheric temperature and pressure on the μ-meson intensity are studied for locations near sea level. The treatment is rigorous in the sense that it includes the continuous production as well as the ionization losses of μ-mesons in the atmosphere. With the help of the newly obtained production spectrum and the exact expression for the survival probability of μ-mesons, a three-term regression formula for the relative changes of μ-meson intensity is derived and discussed in detail. According to this formula, the relative intensity changes are to be correlated not only with the average production height and the ground pressure (a customarily employed two-term correlation) but also with the

average tropospheric temperature. This additional correlation, resulting from the ionization losses of μ-mesons in the air, indicates a possibility of removing some apparent difficulties in the interpretation of experimental data (as, for example, the discrepancies found in the decay coefficients determined from diurnal and seasonal observations, respectively).

(3) The differential energy spectra of π-mesons at production are computed for various geomagnetic latitudes, whereas use is made of the latitude dependence of the production spectrum of μ-mesons. The obtained latitude dependence of the π-meson spectra is linked with the geomagnetic effect on the primary cosmic radiation. Some crude conclusions regarding the multiplicity problem of π-meson production are drawn in a preliminary manner.

TABLE OF CONTENTS

AN ANALYSIS OF THE MESON COMPONENT OF
COSMIC RAYS IN THE ATMOSPHERE

I. INTRODUCTION

Although as yet the origin of the primary cosmic radiation escapes
our knowledge, we believe today that we understand, at least qualitatively,
the secondary phenomena caused in the atmosphere by the primary particles.
Let us recapitulate briefly the sequence of processes which are respon-
sible for all the complexity of the observed local cosmic radiation.

The primary cosmic rays which consist of protons and, to a smaller
extent, α-particles and heavier nuclei, and which are sufficiently ener-
getic to overcome the magnetic field of the earth, reach the upper at-
mosphere from outer space and begin to collide with the oxygen and nitro-
gen nuclei of the air. These nuclear collisions cause not only an ex-
citation and evaporation of the air nuclei, but also an emission of high-
energy secondary nucleons as well as a production of unstable particles,
π-mesons, both charged and neutral.* Neutral π-mesons, having a very
short lifetime (less than 10^{-14} sec) disintegrate immediately into photons,
and thus launch the cascade of photon-electron showers. Charged π-mesons
having also a relatively short lifetime (about 2.7×10^{-8} sec) decay, after
a short distance of travel, into neutrinos and μ-mesons. The latter par-
ticles live on the average 2.1×10^{-6} sec so that they can travel a con-
siderable distance before decaying into neutrinos and electrons. Further-
more, they have exceedingly small cross sections for nuclear interactions
so that their energies can be depleted essentially only by the ionization
losses. Thus in the lower parts of the atmosphere one expects the local
cosmic radiation to be composed primarily of two major components: the
electron-photon component (also called the soft component because of its
absorbability in heavy materials) and the μ-meson component. The third,
nucleonic component, is reduced to a very small fraction of its original
value by nuclear interactions (its absorption mean free path for nuclear
interactions is about 120 g cm^{-2}).

---

* We shall disregard here the heavier mesons since their production rate
  is very small compared with that of π-mesons.

In the following investigations we shall be concerned with the analysis of the μ-meson component of cosmic rays in the atmosphere. This component, due to its relative abundance in the lower atmosphere, is known in its behavior with much greater accuracy than the remaining components mentioned above. There is a sufficient amount of experimental material accumulated throught recent years to provide a reliable basis for the mathematical derivation of a quantity of primary importance to cosmic-ray physics but not accessible by direct measurements: the μ-meson spectrum at production. In addition, there are various observational data which enable one to test the correctness of the assumptions made in the calculations.

However, it is evident already from the crude qualitative picture sketched above that the accurate mathematical equations describing the μ-meson component must necessarily be of complex form. It is, therefore, almost impossible to arrive at usable results without making simplifying assumptions. Furthermore, at some stages of the formulation of the problem one is compelled to make arbitrary assumptions because of the lack of satisfactory theoretical or empirical information. Briefly, even in the case of the relatively well-known μ-meson component one must be aware of the highly limited validity of the obtained results. We shall discuss this problem in more detail in Part II, Sec. B.

We shall base our analysis on a unidimensional model of the differential vertical intensity of μ-mesons, the mathematical form of which was originally considered by M. Sands (SM49). In Part II of this report we shall derive the a priori unknown range spectrum of μ-mesons at production. These calculations will essentially represent repetition of the work carried out by Sands. The necessity for re-calculating the production spectrum arises mainly from the fact that the discrepancies between the early experimental data used by Sands and those obtained more recently with higher accuracy by Conversi (CM50) and others were too serious to be disregarded. Part III deals with the atmospheric effects on the μ-meson intensity near sea level. Using the newly computed production spectrum we shall derive a regression formula for the relative changes of the μ-meson intensity caused by the variations of the atmospheric temperature and pressure. The results obtained will throw a new light on the existing

difficulties in the interpretation of experimental data. Finally, in Parts IV and V we shall touch upon the problems of the latitude dependence of the μ- and π-meson spectra at production. Some crude results will be utilized for speculations on the multiplicity of meson production.

II. RANGE SPECTRUM OF μ-MESONS AT PRODUCTION

A. Notation, Definitions, Units.

In order to avoid repeated explanation of the notations used, we list here the symbols for the physical quantities that will enter into our discussion.

(a) Quantities pertinent to the atmosphere:

x, s — atmospheric depths at the levels of production and observation of μ-mesons, respectively; x and s are equivalent to the atmospheric pressures overhead measured in g cm^{-2} (or approximately in millibars).

x_o — atmospheric depth at sea level; x_o corresponds to the sea-level pressure and its normal value is 1,033 g cm^{-2}.

$\rho(x')$ — air density as a function of atmospheric depth.

$T(x')$ — temperature of the atmosphere as a function of atmospheric depth, measured in absolute units.

(b) Quantities pertinent to the μ-meson:

m_μ = 209 m_e — rest mass of the μ-meson.

τ = 2.10 x 10^{-6} sec — mean life of the μ-meson at rest.

R, R' — residual ranges of μ-mesons at the levels of observation and production, respectively, measured in g cm^{-2} air equivalent.

$c\beta$ — velocity of the μ-meson.

p, U — momentum and total energy of the μ-meson, measured in multiples of $m_\mu c$ and $m_\mu c^2$ respectively.

$k(U)$ — energy loss of μ-meson by collision (ionization loss) measured in multiples of $m_\mu c^2$ per g cm^{-2}.

(c) Quantities pertinent to the μ-meson flux:

$i_v(R, s)$ — differential vertical intensity of μ-mesons; $i_v(R, s) d\omega dR$ represents the number of μ-mesons which arrive at the depth s from the vertical direction within the solid-angle element, $d\omega$, per unit time and unit area, with residual

ranges between R and R + dR; $i_v(R,s)$ is measured in (sec-g-sterad)$^{-1}$. Occasionally the "short-hand" term "intensity" will be used for $i_v(R,s)$.

$I_v(R_o,s)$ - integral vertical intensity of μ-mesons; $I_v(R_o,s)$ is related to $i_v(R,s)$ by the equation:

$$I_v(R_o,s) = \int_{R_o}^{\infty} i_v(R,s)dR, \qquad (1)$$

is, therefore, measured in (sec-cm^2-sterad)$^{-1}$.

(d) Quantities pertinent to the π-meson:

m_π = 276 m_e - rest mass of the π-meson.

τ_π = 2.65 x 10^{-8} sec - mean life of the π-meson at rest.

p_π, U_π - momentum and total energy of π-meson measured in multiples of $m_\pi c$ and $m_\pi c^2$, respectively.

B. Unidimentional Equation for μ-Meson Intensity and its Range of Validity.

Let us attempt to express in mathematical terms the vertical μ-meson intensity which is supposed to develop according to the picture sketched in the Introduction. Consider first the number of charged π-mesons produced by a vertical flux of the N-component (mostly nucleons and π-mesons) in an infinitesimal layer dx at x with total energies between U_π and U_π + dU_π. At a given geomagnetic latitude this number should depend only on the depth x and the energy U_π since the intensity of the N-component does not change noticeably with time and geomagnetic longitude. (We disregard here the abnormal "storms" observed occasionally in the primary radiation.) Now, it is known from the experiments of Tinlot (TJ48) and others that the component producing penetrating showers decreases exponentially with atmospheric depth (this is true at least for the depths between 300 and 1,033 g cm^{-2}). Therefore, if we identify this component with that responsible for the π-meson production, we may write for the number of π-mesons considered above:

$$P(U_\pi)e^{-x/L}dxdU_\pi , \qquad (2)$$

where L is the mean absorption path of the N-component. The function $P(U_\pi)$ may be properly interpreted as the differential energy spectrum of π-mesons at production.

As we shall show below, one may neglect the finite thickness of air traversed by a π-meson before its decay into a μ-meson provided its energy is not exceedingly high. By doing so one can then interpret $P(U_\pi)$ as the differential energy spectrum of π-mesons at decay wherefrom one can obtain directly the differential energy spectrum of μ-mesons at production $M(U)$. According to Ascoli (AG50) this latter quantity is related to $P(U_\pi)$ by:

$$M(U) = \frac{m_\pi m_\mu}{m_\pi^2 - m_\mu^2} \int_{U-}^{U+} P(U_\pi) \frac{dU_\pi}{P_\pi} , \qquad (3)$$

where

$$U_{\pm} = \frac{1}{2} \left(\frac{m_\pi}{m_\mu} + \frac{m_\mu}{m_\pi}\right) \left(1 \pm \frac{m_\pi^2 - m_\mu^2}{m_\pi^2 + m_\mu^2} \beta\right) U \qquad (4)$$

are the upper and lower limits of the energies of π-mesons that can give rise to a μ-meson of energy U (see Fig. 16).

In what follows, it will be more convenient to speak in terms of the differential range spectrum of μ-mesons at production, $G(R')$, rather than in terms of $M(U)$. These two quantities are related by the following equation:

$$G(R') = M(U)\frac{dU}{dR'} = M(U)k(U) . \qquad (5)$$

One can convert one spectrum into the other by making use of the theoretical curves for $k(U)$ and the energy-range relation (see e.g., RB52, Chapter II).

Summarizing, we conclude that the number of μ-mesons produced in dx at x with residual ranges between R' and R' + dR' per sec-cm^2-sterad may be approximated by:

$$G(R')e^{-x/L}dxdR' . \qquad (6)$$

In the above estimate we have neglected the fact that some of the π-mesons as well as some of the μ-mesons will be produced also in directions different from the vertical. However, as we shall see below, for not too low energies these directions will differ only slightly

from the vertical. Accepting this unidimensional model one notes that at the depth of observation the μ-meson arrives with a residual range

$$R = R' - (s-x) , \tag{7}$$

and thus its differential vertical intensity may be written as:

$$i_v(R,s) = \int_0^s G(R+s-x)e^{-x/L} \, w(x,s,R)dx, \tag{8}$$

where $w(x,s,R)$ represents the survival probability of a μ-meson produced at x and arriving at s with a residual range R. The explicit expression for $w(x,s,R)$ will be discussed in Sec. II-D.

Eq. (8) in its formal structure is identical with that investigated by M. Sands (SM49). Since the production spectrum, $G(R')$, is not known (either theoretically or experimentally) Eq. (8) represents an integral equation which one must solve with respect to $G(R')$ by making use of the observational data on $i_v(R,s)$. Before we turn to this problem let us first estimate the residual ranges of μ-mesons for which one may consider Eq. (8) as a reasonable approximation to reality.

In deriving Eq. (8) we have made the following assumptions:

(a) the meson producing component varies exponentially throughout the entire atmosphere;

(b) the air layer traversed by π-mesons before their decay is infinitesimally small;

(c) the production of π-mesons and μ-mesons is collimated along the vertical;

(d) the multiple scattering of μ-mesons in the air is negligible.

Among all the above assumptions the assumption (a) is probably the most arbitrary one. Although it is empirically justified for high-energy events at atmospheric depths below the 300-mb level, it is quite uncertain that the same exponential law should hold for lower energies and for depths above 300 mb. We are forced to make this assumption here because of the lack of any better information. The errors introduced thereby cannot be estimated rigorously. One might only remark that the error should not be too serious if the significant deviations occur only above 100 mb (this is so because the contributions to the μ-meson intensity originate mostly from the layers below that level).

Concerning the assumption (b) one readily verifies that it represents a good approximation if the momentum of π-mesons is not exceedingly high. The mean free path of a π-meson before decay is given by:

$$L_d = c \, \widetilde{\tau}_\pi \, \varrho(x) p_\pi \approx 10^{-3} p_\pi x \qquad (\text{g cm}^{-2}) \qquad (9)$$

which is of the order of a few grams per cm^2 for π-mesons produced in the proximity of 100-mb level with momentum smaller than $100 \, m_\pi c$. For momenta larger than this value L_d becomes comparable with the geometric mean free path of π-mesons for nuclear interaction, and the assumption that almost all π-mesons decay into μ-mesons before interacting with air nuclei is no longer valid. We shall take the value of $p_\pi = 100$, which corresponds to the μ-meson range of about $6,000 \, \text{g cm}^{-2}$, as the upper limits for the validity of Eq. (8).

In contrast to the limitations on Eq. (8) arising from the assumption (b) the assumptions (c) and (d) impose a lower limit upon the range of validity of Eq. (8). The assumption on the collimation of π-mesons produced in nuclear interactions is essentially based on the relativistic contraction of their cone of emission in the laboratory system. The numerical value of the maximum angle of emission with respect to the line of flight of the primary particle depends on the angular distributions of π-mesons in the center-of-mass system. Since the present knowledge on this problem is only of a speculative character, it is impossible to make an accurate estimate of the errors involved. However, the experimental observations in photographic emulsions at high altitudes (BRH49) clearly indicate that most of the π-mesons with minimum ionization (thin secondary tracks) are emitted in the laboratory system at angles smaller than 15° with respect to the direction of the primary particle. This empirical fact may be considered as sufficient to support the assumption on the collimation of π-mesons provided one considers π-mesons with momenta larger than about $2m_\pi c$ (threshold value for minimum ionization).

The maximum angle of emission of μ-mesons in the decay process of π-mesons can be readily calculated and is given by:

$$\sin \vartheta_{max} = \frac{1}{2}\left(\frac{m_\pi}{m_\mu} - \frac{m_\mu}{m_\pi}\right) \frac{1}{p_\pi} = \frac{0.282}{p_\pi} \, ; \quad (p_\pi \geq 0.282). \qquad (10)$$

Hence ϑ_{max} is smaller than 8° for $p_\pi > 2$.

The effect of the multiple scattering of μ-mesons may be best estimated from the magnitude of the mean-square angle which is given by:

$$\left\langle \theta^2 \right\rangle_{AV} = \frac{1}{X_o}\left(\frac{E_s}{m_\mu c^2}\right)^2 \int^s \frac{dx'}{\beta^2 p^2} = \frac{1}{X_o}\left(\frac{E_s}{m_\mu c^2}\right)^2 \int_{(\beta p)_s}^{(\beta p)_x} \frac{d(\beta p)}{\left[-\frac{d(\beta p)}{dx'}\right]\beta^2 p^2} . \tag{11}$$

($E_s = 21$ Mev; $X_o = 38$ g cm^{-2}, see RB52, Chapter II). The quantity

$$-\frac{d(\beta p)}{dx'} = (1 + \frac{1}{U^2})k(U)$$

appearing in the denominator of the integrand in Eq. (11) is practically constant for all $p > 2$ (its numerical value for air is 2.1×10^{-2} g^{-1}cm^2) so that one has the following simple formula for the mean-square angle:

$$\left\langle \theta^2 \right\rangle_{AV} = 0.050 \left(\frac{1}{(\beta p)_s} - \frac{1}{(\beta p)_x} \right) . \tag{12}$$

Eq. (12) implies, for example, that a μ-meson produced at 100-mb level and arriving at sea level with $p = 3$ will have a rms angle of 7.0^o. For momenta smaller than this value the deviations from the vertical become more critical.

Summing up we see that, if we exclude μ-mesons with momenta smaller that $3\,m_\mu c$ (corresponding range 100 g cm^{-2}) we may expect that the local μ-meson intensity, produced by a vertical flux of the N-component, will be contained within a vertical cone of 30° zenith angle. The uni-dimensional treatment of the development of the μ-meson component can be considered valid within these limits.

Referring to the latter limitation and to the limitation arising from the assumption (b), we conclude that the range interval in which Eq. (8) represents a reasonable approximation to reality extends from $R = 100$ g cm^{-2} up to $R = 6,000$ g cm^{-2} air equivalent.

C. Experimental Information Concerning the μ-Meson Component.

As we have mentioned in the foregoing section, Eq. (8) can be solved with respect to the range spectrum at production only if one has at his disposal a sufficient amount of experimental data concerning the μ-meson intensity, $i_v(R,s)$. We have chosen the following two experiments as the most reliable and suitable for the purposes of our analysis.

      (a) measurements of the differential distribution-in-momentum of cosmic-ray mesons at sea level by Caro, Parry and Rathgeber (CDR50);

      (b) measurements of the altitude dependence of cosmic-ray mesons with residual ranges between 100 and 117 g cm^{-2} air equivalent by M. Conversi (CM50).

In the first experiment the penetrating cosmic-ray particles coming nearly from the vertical direction (the opening angle was about 16°) were deflected in the air gap of an electromagnet and the deflection was recorded by means of an array of G.M. counters. The measurements were carried out at sea level and covered the momentum range between 2.4×10^2 and 5×10^4 Mev/c. The differential momentum spectrum thus obtained is reproduced in Fig. 1. Since the particles recorded represent almost exclusively the vertical μ-mesons, one can utilize the above data for reconstructing the differential vertical intensity of μ-mesons at sea level, $i_v(R,x_o)$, as a function of the residual range R. Applying the theoretical expression for the momentum loss, k/β, for μ-mesons in air we arrived at a curve shown in Fig. 2. The solid line corresponds to the measurements by Caro et al, while the dashed line represents Rossi's curve (RB48) drawn for comparison. Note significant deviations from Rossi's curve at residual ranges above 3,000 g cm^{-2}.

In addition to the above sea-level data, we shall find the measurements by Conversi as indispensable for studies concerning the behavior of the production spectrum at small residual ranges. Combining the techniques of delayed coincidences and anticoincidences, Conversi was able to determine the absolute number (per sec-g-sterad) of μ-mesons stopped in 10 cm of graphite after traversing 15.2 cm of lead for various atmospheric depths at 50° N geomagnetic latitude. The counter telescope had a relatively good geometry (the maximum zenith angle permitted for a meson entering the telescope and stopping in the absorber was about 35°)
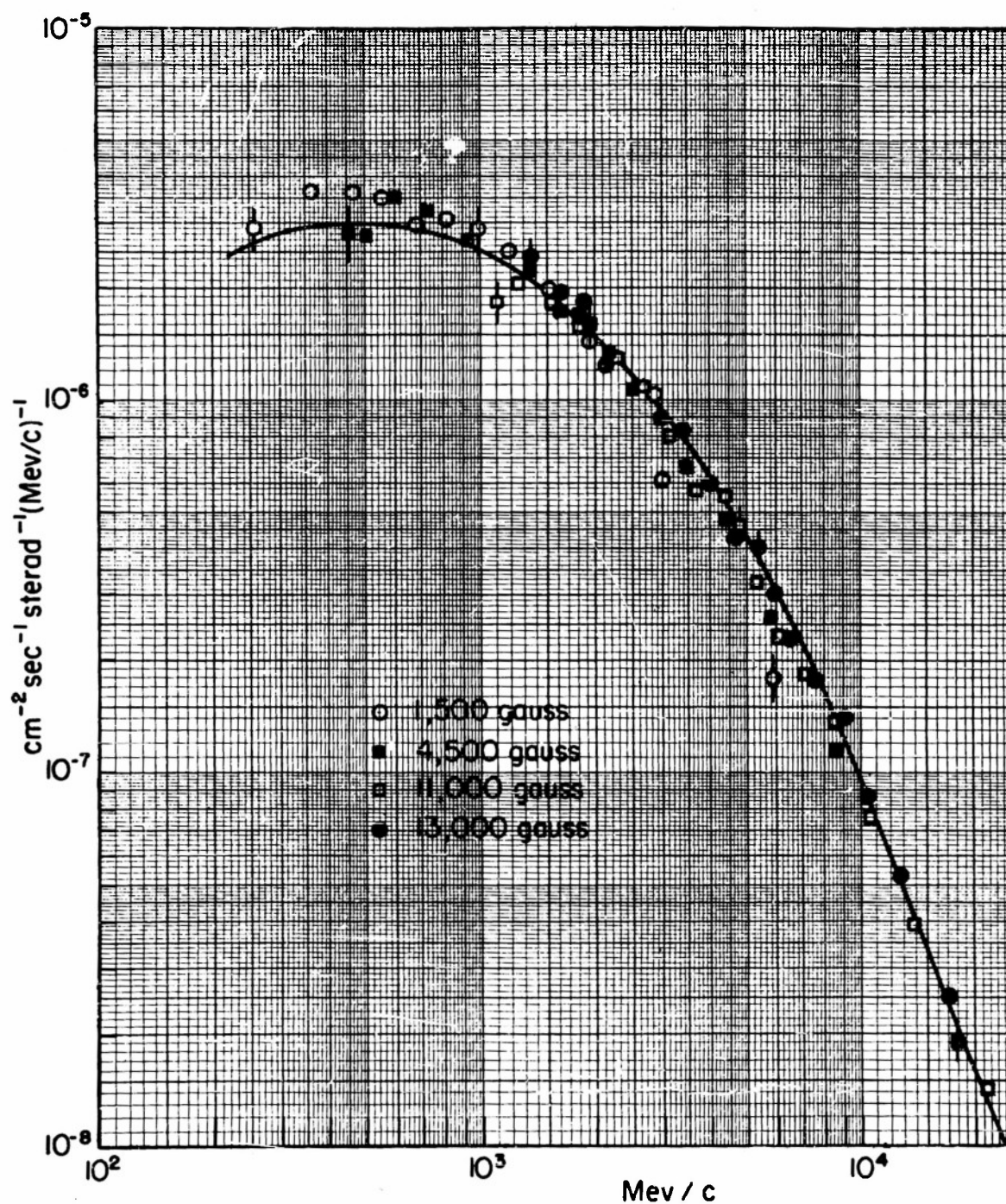
Figure 1

Differential momentum distribution of μ-mesons
at sea level measured by Caro et al. (CDE50).

Figure 2

Vertical differential intensity of
μ-mesons at sea level, $i_v(R,x_o)$, as
a function of residual ranges, R,
measured in g cm^{-2} air equivalent,
computed from Caro's data (CDE50).
The dashed line represents Rossi's
curve (RB48). The open circles rep-
resent the $i_v(R,x_o)$-values computed
on the basis of equations (II-8) and
(II-33).
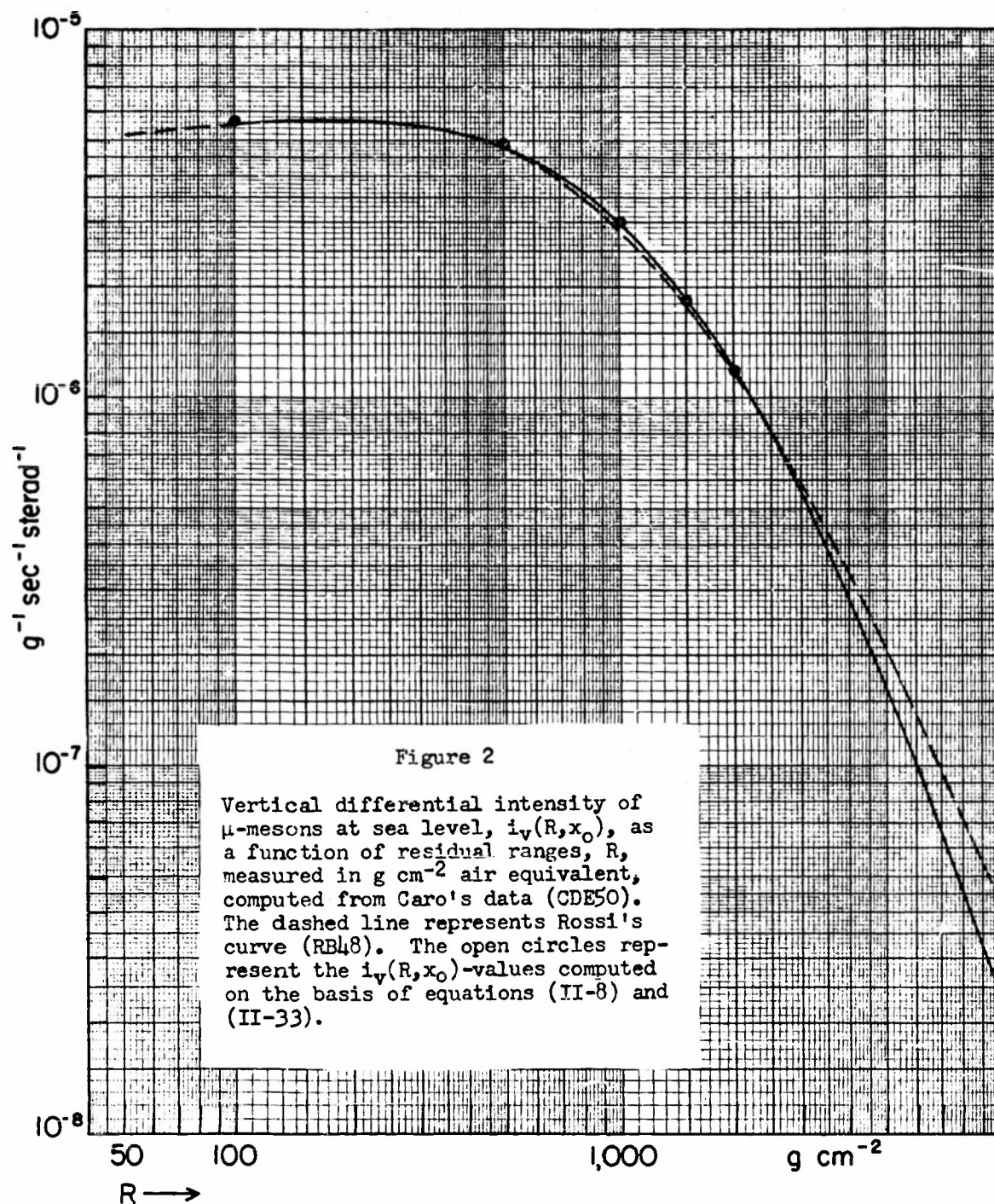
and the statistical accuracy of the data exceeded that of earlier measurements of this kind (RB47, SM49) considerably. The delay curves yielded a mean life which was consistent with that of μ-mesons at all depths considered. Thus one may interpret Conversi's data as a direct measure for the dependence of the vertical differential intensity on the atmospheric depth for a μ-meson with residual ranges between 100 and 117 g cm^{-2} air equivalent. Conversi's results with corresponding errors are shown in Fig. 3; the solid line represents the differential vertical intensity as computed on the basis of the production spectrum derived in Sec. II-E. The dashed line represents the normalized intensity-depth curve deduced by Sands (SM49) from his earlier measurements. The large difference in the behavior of Sands' and Conversi's curves, respectively, is primarily due to the fact that Sands' data cannot be interpreted as directly representative for the vertical differential intensity of μ-mesons. They rather represent an intensity integrated not only over all ranges of mesons between 5 and 83 g cm^{-2} but also over all directions of incidence (the opening angle of Sands' arrangement was close to 180°).

Concluding, we would like to call the reader's attention to the good agreement existing between the measurements of Caro et al. and those of Conversi for μ-mesons at sea level with residual ranges of 100 g cm^{-2}. (Note that both experiments were performed at geomagnetic latitudes near 50° although on opposite sides of the geomagnetic equator.)

D. Survival Probability of μ-Mesons.

Another quantity which enters into our basic equation (8) is the survival probability of μ-mesons, $w(x,s,R)$. Due to its implicit dependence on the vertical distribution of the atmospheric temperature, this quantity will be treated separately in some detail.

For a μ-meson, produced at the elevation z, which travels vertically toward the earth with the velocity cβ and is observed at the elevation z_o the survival probability is given by:

$$w = \exp\left[-\int_z^{z_o} \frac{\sqrt{1-\beta^2}}{c\,\tau\,\beta}\,dz'\right] ; \tag{13}$$

Figure 3

Vertical differential intensity of
μ-mesons with residual ranges be-
tween 100 and 117 g cm⁻² air equiv-
alent as a function of atmospheric
depth at 50° N geomagnetic latitude.
The full circles, with corresponding
errors, represent the measurements
of Conversi (CM50); the open circle
represents the measurements of Krau-
shaar (KW49) at Echo Lake. The
dashed line represents Sands' mea-
surements on μ-mesons with residual
ranges between 5 and 83 g cm⁻². The
solid curve was computed by means of
Eqs. (II-32) and (II-33).

the factor $\sqrt{1-\beta^2}$ in Eq. (13) accounts for the relativistic time dilata-
tion. It is convenient to express the distance element, dz', in terms
of the increment, dx', of the atmospheric depth. Since $dx' = \rho(x')dz'$
Eq. (13) may be written as:

$$w(x,s,R) = \exp\left[-\frac{1}{c\tau}\int_x^s \frac{dx'}{\rho(x')p'}\right].$$ (14)

Here p' stands for the momentum of the μ-meson at the depth x' expressed
as a function of the corresponding residual range (R + s - x').

We shall find it useful for the consideration in Part III to ap-
proximate the momentum-range relation by the following analytical formula:

$$\frac{1}{p} = \frac{B}{b+R} - \mathcal{K},$$ (15)

where $B = 53.5$ g cm^{-2}; $b = 56$ g cm^{-2} if R is measured in g cm^{-2} air
equivalent; $\mathcal{K} = $ constant $= 2.07 \times 10^{-3}$. With the numerical values of the
constants quoted above, Eq. (15) is applicable for all μ-mesons with resi-
dual ranges between 30 and 6,000 g cm^{-2} air equivalent. In this region
it reproduces the theoretical curve (RB52, pages 40-41) within an accuracy
of one percent. Referring to the discussion of the validity of Eq. (8) in
Sec. II-B we may consider Eq. (15) as sufficient for the purposes of our
analysis.

The evaluation of Eq. (14) also requires the knowledge of the
vertical behavior of the air density, $\rho(x')$ or of the atmospheric tem-
perature, T(x'). These two quantities are related by the following
equation:

$$\frac{x'}{\rho(x')} = \frac{\mathcal{R}T(x')}{\overline{M}g}$$ (16)

where $\mathcal{R}$ is the universal gas constant, $\overline{M}$ is the mean molecular weight
of air, and g is the acceleration of gravity ($\mathcal{R}/Mg = 2.87 \times 10^3$ cm/$^\circ$C).
It is more appropriate to discuss the survival probability in terms of
T(x') rather than in terms of $\rho(x')$ because T(x') is a quantity that
can be measured directly by means of radiosondes.

By combining Eqs. (14), (15) and (16) one can write for the
survival probability:

$$w(x,s,R) = \exp\left[-\frac{\mathcal{R}}{c\tau \bar{M}g}\int_x^s \frac{T(x')}{x'}\left(\frac{B}{x_e-x'}-\mathcal{U}\right)dx'\right], \tag{17}$$

where we have put for short:

$$x_e = R + s + b.$$

Since:

$$\frac{1}{x'(x_e-x')} = \frac{1}{x_e}\left[\frac{1}{x'}+\frac{1}{x_e-x'}\right] \quad ,$$

the following representation of $w(x,s,R)$ is possible:

$$w(x,s,R) = \exp\left[\alpha_H(s,R)H(x,s) + \alpha_K(s,R)K(x,s,R)\right], \tag{18}$$

where

$$\alpha_H(s,R) = \frac{-1}{c\tau}\left(\frac{B}{x_e}-\mathcal{U}\right) = -\frac{1}{c\tau p(s+R)} \quad ; \tag{19}$$

$$\alpha_H(s,R) = -\frac{D}{\bar{M}gc\tau x_e^2} \quad , \tag{20}$$

and

$$H(x,s) = \frac{\mathcal{R}}{\bar{M}g}\int_x^s \frac{T(x')}{x'}dx' \quad , \tag{21}$$

$$K(x,s,R) = x_e\int_x^s \frac{T(x')}{x_e-x'}dx' \quad . \tag{22}$$

The representation of $w(x,s,R)$ given by Eq. (18) has some advantages over those given by Eqs. (14) or (17). The two terms in the exponent of Eq. (18) have a direct physical significance. The function $H(x,s)$ defined by Eq. (21) represents simply the distance from the pressure level x (the production level) to the pressure level s (the observation level).

The first term in Eq. (18), $\exp(\alpha_H H)$, is the main term; it represents the survival probability for a μ-meson produced at x and traveling the distance H with a __fixed__ momentum $p(s + R)$. For most of the mesons recorded in the lower atmosphere, x is considerably smaller than s so that $p(s + R)$ will not differ significantly from the actual momentum at production $p(s + R - x)$. This implies that approximately

$$\exp(\alpha_H H) \approx \exp\left[-\frac{H}{c\tau p(s+R-x)}\right].\qquad(23)$$

One recognizes in the right-hand side expression a formula that is often quoted in the literature. It represents the survival probability of μ-mesons if one neglects their ionization losses in the air.

The second term in Eq. (18), $\exp(\alpha_K K)$, may be regarded as a corrective term accounting for the ionization losses of μ-mesons in the air. The function $K(x,s,R)$ defined by Eq. (22) will, in general, depend not only on the temperature distribution but also on the residual range of the μ-meson under consideration. However, for sufficiently large R (say, $R > 1,000$ g cm^{-2}) $K(x,s,R)$ may be written roughly as

$$K(x,s) = \int_x^s T(x')dx' = \frac{\bar{M}g}{\mathcal{R}}\int_{z_0}^z x'dz,\qquad(24)$$

i.e., in case of fast mesons, the function K is closely related to the temperature averaged over the region between the levels of production and observation or, what is equivalent, to the amount of air mass overhead.

For the numerical evaluation of Eq. (18) one needs the meteorological data on $T(x')$ which, in general, will be different for different seasons, different geographic locations, etc. However, a closer study of meteorological data shows that for the description of the __annual means__ of atmospheric temperature one needs essentially only two parameters: the atmospheric depth (i.e., the pressure overhead) and the geographic latitude. The longitudinal variations of the annual means at a given latitude circle turn out to be insignificant except for the localities

with extreme weather conditions as, e.g., localities with a pronounced continental or maritime climate. Even in those exceptional cases the deviations become significant only in the lower parts of the troposphere. Hence, it is plausible to consider the annual means of $T(x')$ averaged along a given latitude circle as basic quantities. The local corrections may be then carried out with the aid of a regression formula. An explicit expression of such a formula will be discussed at length in Part III of this report. Here we shall be merely concerned with the annual means of $T(x')$. Fig. 4 shows the behavior of these means plotted as functions of the atmospheric depth for various geographic latitudes. Th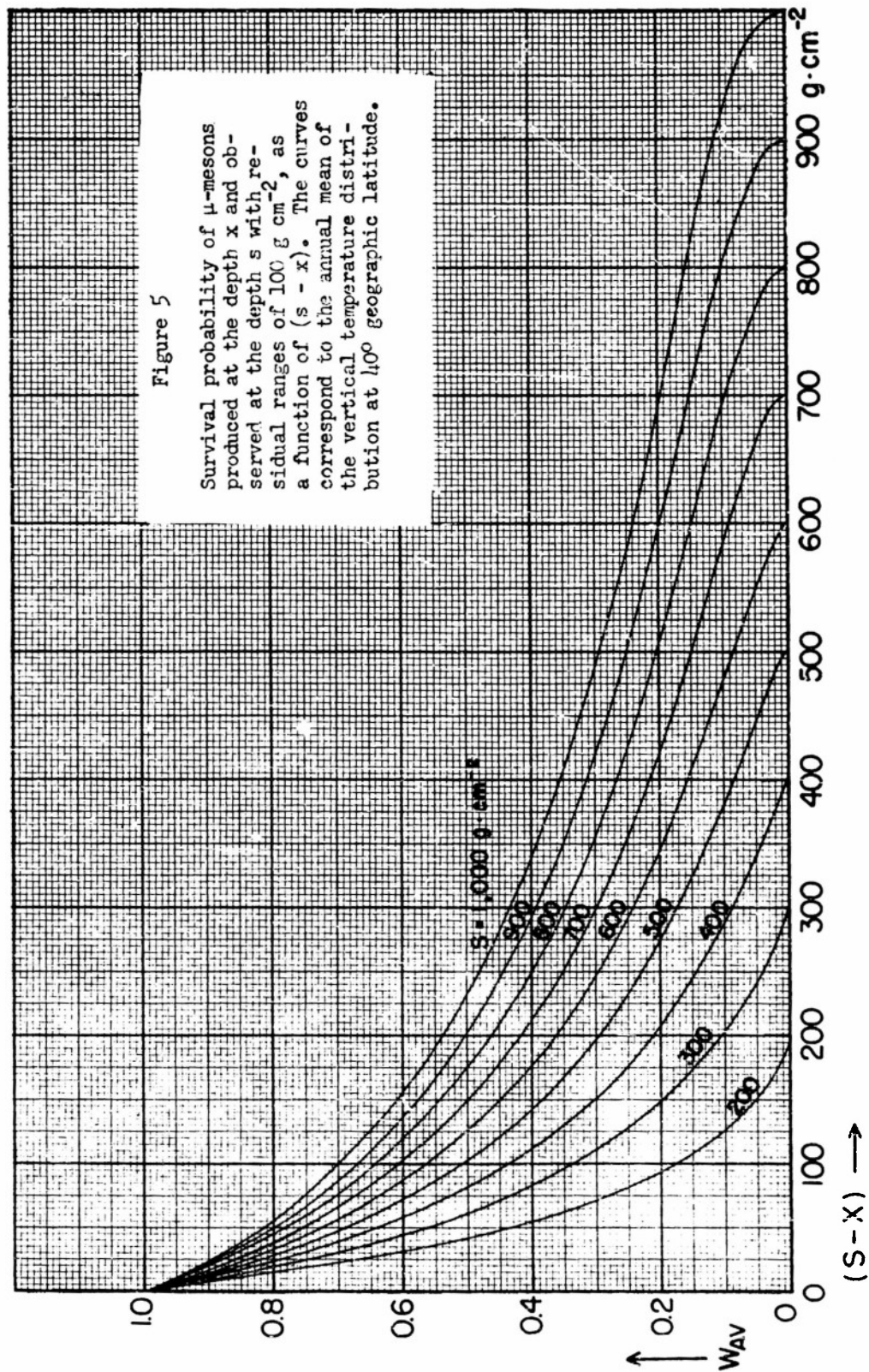e curves were constructed from a graph given by Haurwitz and Austin in their textbook on climatology (HB44, page 37). Note the inverse behavior of the temperature in the stratosphere and the troposphere when one passes from the equatorial region to the middle latitudes. The temperature distribution in the upper stratosphere (above 10 mb) is not as yet definitely known; however, this uncertainty does not affect our considerations noticeably.

By means of Eq. (18) and Fig. 4 one can calculate numerically the average survival probability for any given latitude. Since the experiments of Conversi and Caro et al. were carried out in the proximity of 40° geographic latitude, we based our calculations on the temperature distribution of this region. Referring to the experiment of Conversi we show in Fig. 5 the survival probability for μ-mesons produced at the depth x and observed at the depth s with residual ranges of 100 g cm^{-2} $\left[w(x,s,100)\text{ is plotted }\underline{\text{versus}}\text{ the amount of air traversed, }s\text{-}x\right]$. Referring to the experiment of Caro et al. we show in Fig. 6 the negative natural logarithm of survival probability for μ-mesons produced at x and reaching sea level with various residual ranges between 100 and 2,000 g cm^{-2}. Regarding the μ-mesons which arrive at sea level with residual ranges larger than 2,000 g cm^{-2}, it is useful to approximate their survival probability by the following simple formula:

$$w(x,x_0,R) = v(R)\left(\frac{x}{x_0}\right)^{\lambda(R)} , \qquad (25)$$

where the quantities $v(R)$ and $\lambda(R)$ are numerically derived functions of the residual ranges at sea level and are shown in Fig. 7. The right-hand side expression in Eq. (25) reproduces the survival probability

Figure 4

Vertical distribution of the annual means of temperature as functions of atmospheric depth at various geographic latitudes, computed from the graph given by Haurwitz and Austin (HB44, page 37).

Figure 5

Survival probability of μ-mesons produced at the depth x and observed at the depth s with residual ranges of 100 g cm⁻², as a function of (s - x). The curves correspond to the annual mean of the vertical temperature distribution at 40° geographic latitude.

Figure 6

Negative natural logarithm of survival probability for μ-mesons produced at the depth x and reaching sea level with various residual ranges between 100 and 2,000 g cm⁻². The curves correspond to the annual mean of the vertical temperature distribution at 40° geographic latitude.
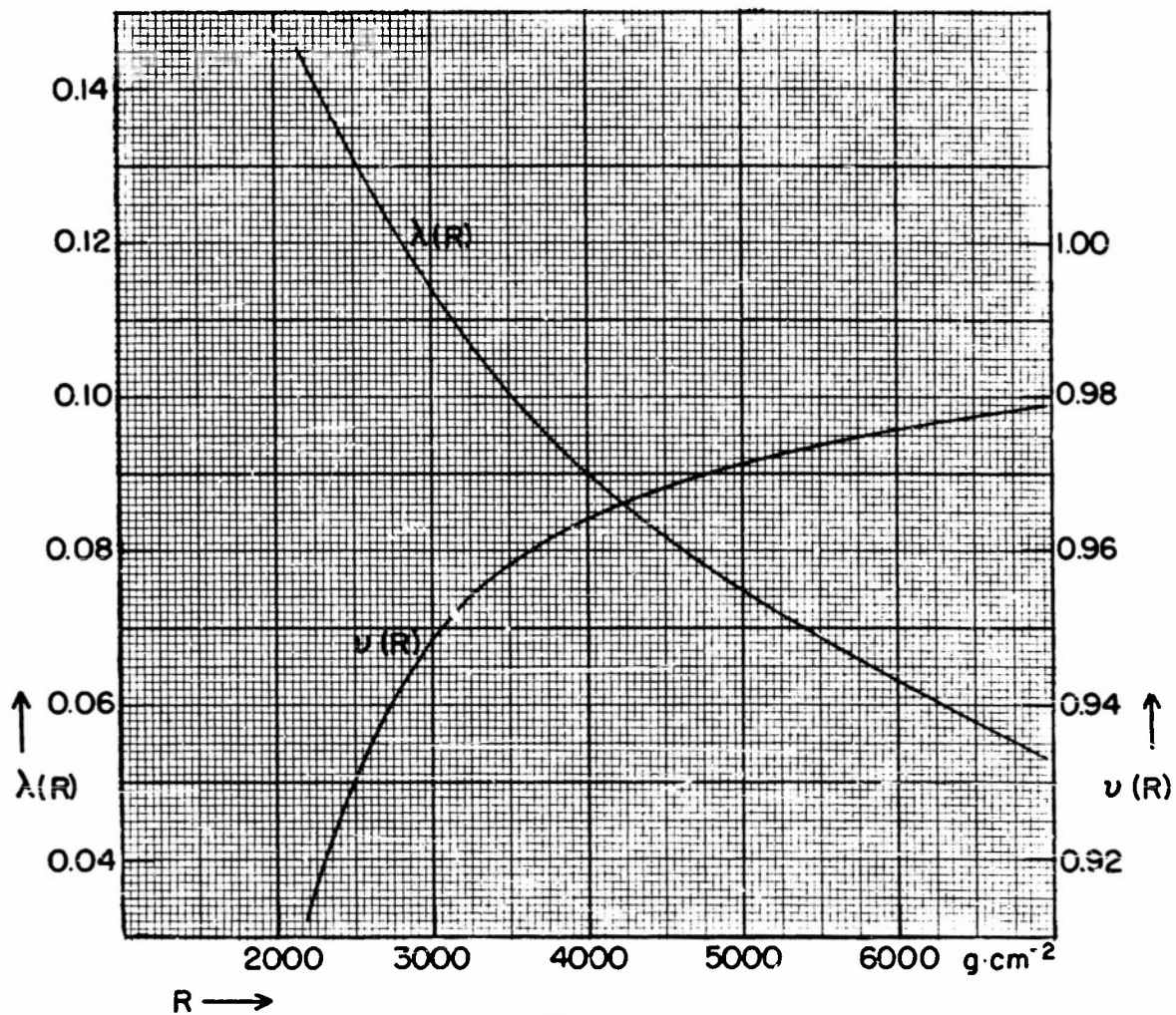
Figure 7

The functions $v(R)$ and $\lambda(R)$ describing the
survival probability of fast μ-mesons at sea
level, viz: $w(x,x_0,R) = v(R) \, (x/x_0)^{\lambda(R)}$.

very accurately for all production levels with $x < 500$ g cm^{-2}; at production levels closer to the ground (contributing very little to the value of Eq. (8)) the formula (25) introduces errors which amount only to a few percent of the actual values of $w(x,x_o,R)$. It is interesting to compare Eq. (25) with the survival probability of fast mesons in the case of the isothermal atmosphere. The latter probability may be obtained directly from Eqs. (21) and (23) by setting T = constant; then:

$$w_{isothermal} = (\frac{x}{x_o})^{\mathcal{R}T/c\tau \bar{M}gp} . \tag{25'}$$

The resemblance between Eqs. (25') and (25) is emphasized by the fact that the function $v(R)$ does not depart markedly from unity, and the function $\lambda(R)$ behaves similarly to the expression $\mathcal{R}T/c\tau Mgp(x_o+R)$.

E. Solution of the Intensity Equation with Respect to the Production Spectrum.

We are now prepared to turn to our main problem: the solution of Eq. (8) with respect to the range spectrum of μ-mesons at production. Following the procedure of Sands (SM49) we find it convenient to begin with the determination of $G(R')$ at large values of residual ranges.

(a) Production spectrum at large residual ranges.
If one considers the μ-meson intensity only for large ranges at sea level (say, $R > 2,000$ g cm^{-2}) one can introduce two simplifications in Eq. (8); first, one can express the survival probability in terms of Eq. (25), second, one can assume the production spectrum, $G(R')$, to be a slowly varying function within the interval of integration. The latter assumption is justified by the fact that, for large R, the residual range at production, $R' = R+x_o-x$, does not change strongly within the interval $0 \leqslant x \leqslant x_o$. The slow variation of $G(R')$ suggests the application of the mean value theorem of integral calculus to the right-hand side of Eq. (8). According to the discussion in the Appendix one has then

$$i_v(R,x_o) = G(R+x_o-x_m) \int_0^{x_o} e^{-x/L} w(x,x_o,R)dx. \tag{26}$$

The substitution of Eq. (25) yields for Eq. (26)

$$i_v(R,x_o) = G(R+x_o-x_m)Lw(L,x_o,R)\Gamma(1+\lambda;x_o/L) , \tag{27}$$

where

$$\Gamma(z;y) = \int_0^y t^{z-1} e^{-t} dt \xrightarrow[y\to\infty]{} \Gamma(z) - y^{z-1} e^{-y} \qquad (28)$$

is the incomplete gamma function. Due to the fact that x_0/L is considerably larger than one, one can approximate $\Gamma(1+\lambda \,; x_0/L)$ by the complete gamma function, $\Gamma(1+\lambda)$. The value of the "mean" depth x_m can be estimated with the aid of Eq. (A-2); one finds thus:

$$x_m = \frac{\Gamma(2+\lambda \,; x_0/L)}{(1+\lambda \,; x_0/L)} L \approx (1+\lambda)L . \qquad (29)$$

Hence, referring to Eqs. (27) and (29), one has the following approximate solution for the production spectrum at large ranges:

$$G(R+x_0-x_m) = \frac{i_v(R,x_0)}{Lw(L,x_0,R)\Gamma(1+\lambda)} . \qquad (30)$$

Taking for the absorption mean free path, L, the numerical value of 121 g cm^{-2} and using Figures 2 and 7, we have computed $G(R+x_0-x_m)$ for 2,000 g cm$^{-2} < R < 6,000$ g cm^{-2}. The resulting curve is shown in Fig. 8. At first sight this curve seems to be expressible in terms of a simple power law. However, a closer inspection shows that the following representation is more accurate:

$$G(R') = \frac{C}{(a+R)^\gamma} \qquad (31)$$

where C, a and γ are positive constants. Unfortunately, the range interval for which Eq. (30) is valid is too small to permit an unambiguous choice of a unique set of the three constants C, a, and γ. One can readily verify that it is possible to reproduce the curve in Fig. 8 by assuming any arbitrary value between 200 and 700 g cm^{-2} for the constant a, if the remaining constants, C and γ, are properly adjusted. Table I gives four such sets of the numerical values of C, a, and γ, which reproduce the spectrum curve in Fig. 8 equally well. Of course, any set of constants obtained by an interpolation of the values quoted in Table I is also compatible with our solution Eq. (30).
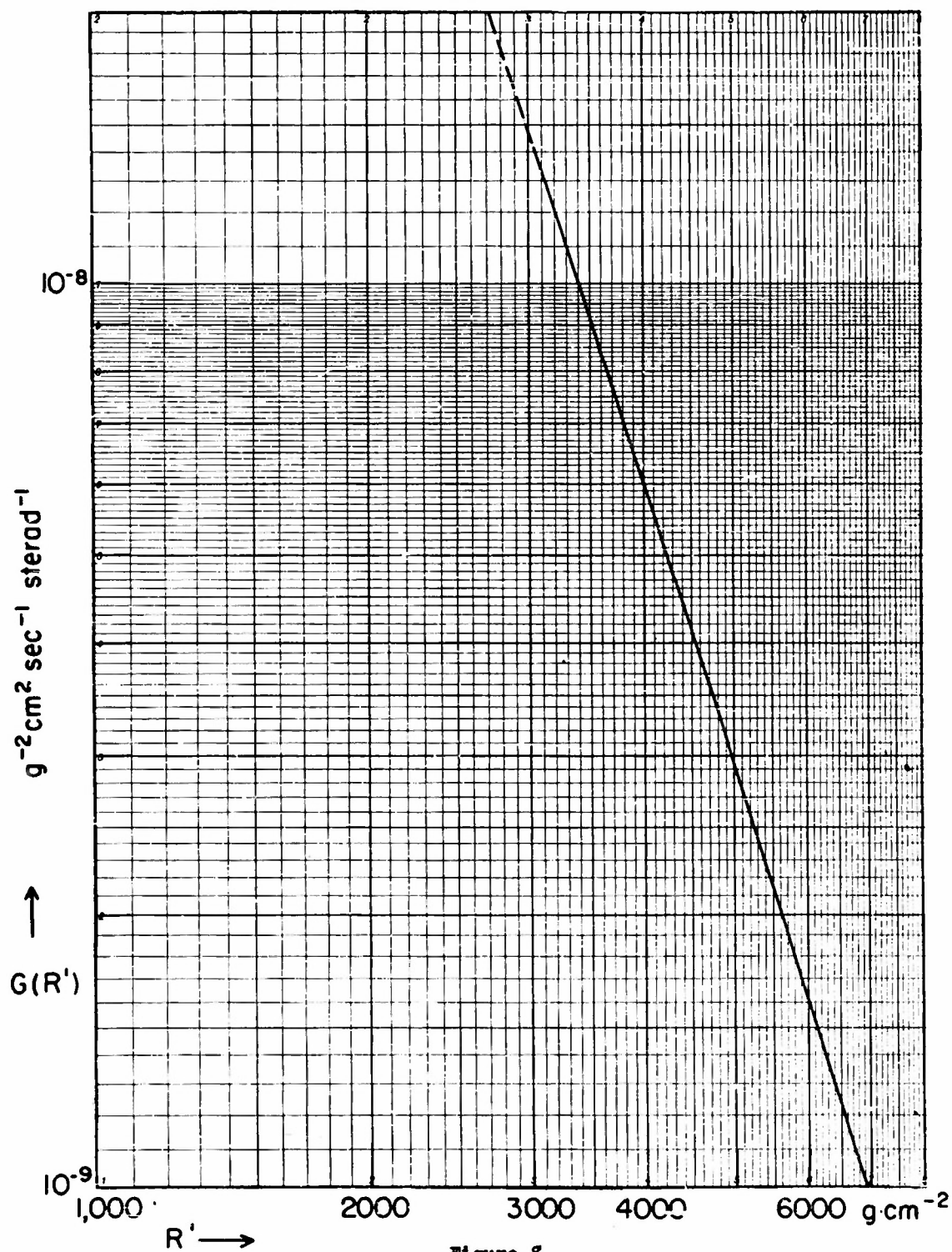
Figure 8

Range spectrum of μ-mesons at production for
large residual ranges.

TABLE I

Four sets of constants, a, γ, and C, which are equivalent for the empirical representation of the production spectrum of μ-mesons at residual ranges larger than 3,000 g cm^{-2} air equivalent:

$$G(R') = C(a+R')^{-\gamma}.$$

Set No.	a (g cm^{-2})	γ	C (g$^{\gamma-2}$cm$^{2-2\gamma}$ sec^{-1}sterad^{-1})
1.	300	3.46	2.25×10^4
2.	400	3.51	3.30×10^4
3.	500	3.57	6.61×10^4
4.	600	3.63	11.84×10^4

In order to eliminate this ambiguity one must turn to the region where
the residual range at production assumes values comparable with those
permitted for the constant a, i.e., smaller than 1,000 g cm^{-2}. Evi-
dently, the μ-meson intensities measured by Conversi correspond to such
a region. Thus, by making use of Conversi's data one can test if the pro-
duction spectrum at small ranges is expressible by a formula suggested
from the large-range data and, if so, to determine a unique set of values
for the characteristic constants.

(b) Production spectrum at small residual ranges.

According to the discussion in the foregoing sections we may trans-
late the data of Conversi into the following equation:

$$i_v(100,s) = \int_0^s G(100+s-x) \; e^{-x/L} \; w(x,s,100)dx \, , \quad (32)$$

where the survival probability is given by Fig. 5.

Assuming that the production spectrum, $G(100+s-x)$, is expressible
by Eq. (31) we have evaluated numerically the right-hand side of Eq. (32)
for various depths s ranging between 200 and 1,000 g cm^{-2}. The calcula-
tions were repeated four times, each time with a different set of con-
stants a, C, and γ quoted in Table I. The results thus obtained were
then compared with the experimental points given in Fig. 3. Among the
computed curves, the one corresponding to the third set of constants
$(a = 500$ g $cm^{-2}, \gamma = 3.57$, C = 6.61 x $10^4)$ was found to be in closest
agreement with the experimental data. When a set of constants obtained
by an interpolation between the third and fourth sets of Table I was
taken, the agreement became practically complete except for one point
at the depth of 231 g cm^{-2} (see the solid line in Fig. 3). Conversi's
value of the μ-meson intensity at this depth falls above the calculated
curve. We believe, however, that this measurement should be corrected
for the μ-mesons locally produced in the lead absorber by the nucleons
which are still abundant at this high altitude (for remarks on this
problem see also CM50). Corrections of this kind may be expected to be
of the order of 20 percent. Therefore, we do not consider this single
discrepancy as crucial.

Summarizing, we conclude that the following expression for the μ-meson spectrum at production:

$$G(R') = \frac{7.31 \times 10^{4}}{(520 + R')^{3.58}} \qquad \left[g^{-2}cm^{2}sec^{-1}sterad^{-1}\right] \qquad (33)$$

is compatible with the experimental data for residual ranges between 100 and 1,100 g cm^{-2} (Conversi's data), and 3,000 and 6,000 g cm^{-2} (Caro's data). In order to test the compatibility of the above formula also for the intermediate ranges between 1,000 and 3,000 g cm^{-2} it is sufficient to calculate the values of the differential intensity of μ-mesons which arrive at sea level with residual ranges between 100 and 2,000 g cm^{-2} and to compare the results with Fig. 2. This has been done numerically by using the graphs in Fig. 6 for the survival probability. The computed points are indicated by open circles in Fig. 2. One sees that the agreement is fully satisfactory.

In Fig. 9 we show the μ-meson spectrum at production computed from Eq. (33) for small and intermediate ranges; the dashed curve represents the production spectrum as derived by Sands. It is interesting to note that our smooth production spectrum behaves in such a way as to average out the "dip" obtained by Sands at $R' = 100$ g cm^{-2}.

We close the discussion of this part of our analysis with a few remarks concerning the degree of accuracy that one may claim for Eq. (33). Since, for $2,000 < R < 6,000$ g cm^{-2}, Eq. (33) is equivalent to Eq. (30) we can estimate the relative error made in our computation of G at large ranges by means of Eq. (A-4), viz:

$$\text{relative error} = \frac{1}{2}(1+\lambda)L^{2}\left[\frac{1}{G}\frac{d^{2}G}{dR'^{2}}\right]_{R' = R+x_{o}-x_{m}}$$

$$= \frac{1}{2}\gamma(1+\gamma)(1+\lambda)\left[\frac{L}{a+R+x_{o}-x_{m}}\right]^{2}.$$

For $R > 2,000$ g cm^{-2} this error is smaller than 1.2 percent. Hence, referring to Eq. (30), at large residual ranges one may consider the production spectrum to be known almost as accurately as the μ-meson intensity at sea level itself. It is more difficult to estimate the errors contained

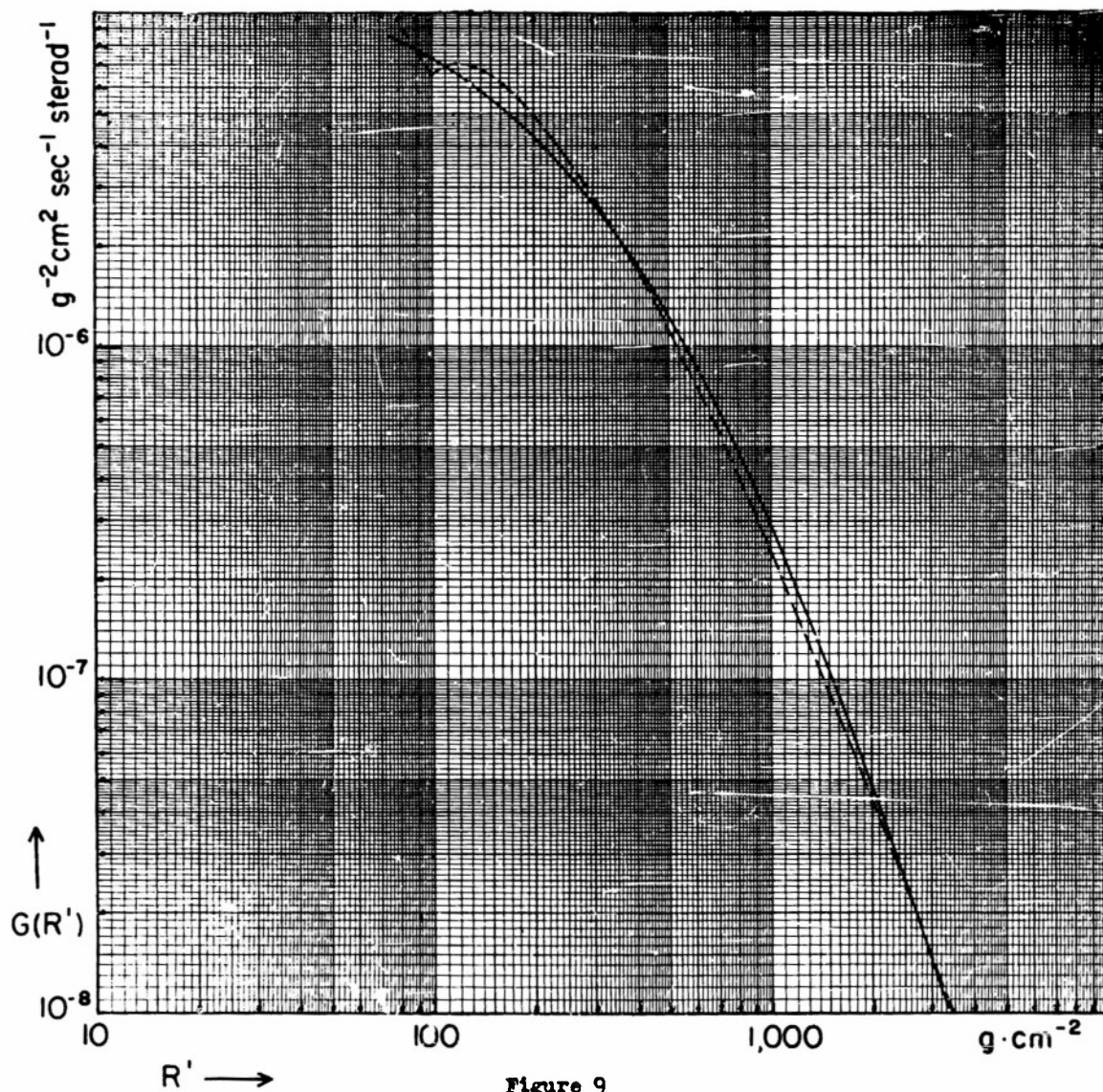Figure 9

Range spectrum of μ-mesons at production for small and intermediate residual ranges. The dashed curve represents the production spectrum derived by Sands (SM49). The solid curve was computed from Eq. (II-33)

in the determination of G at small ranges. However, the accuracy with
which the constant a is known can be taken as a good measure for the
uncertainties involved. Our repeated evaluations of Eq. (32) for dif-
ferent values of a showed that $i_v(100,s)$ is quite sensitive to the assumed
values of this constant. For example, a 5 percent uncertainty in $i_v(100,s)$
at $s = 300$ g cm^{-2} produced only a 2 percent uncertainty in a. Since the
exponent γ is relatively insensitive to the values of a (see Table I) and
is essentially determined by large-range measurements, one can regard ex-
pression (33) for the production spectrum at $50°$ geomagnetic latitude as
comparatively well established.

III. ATMOSPHERIC EFFECTS ON μ-MESON INTENSITY NEAR SEA LEVEL

A. General Remarks.

Numerous experiments* of the last two decades have shown that the
intensity of cosmic rays is influenced by the atmospheric conditions
existing during the period of observation. It has been found from ex-
periments on the ground that the variations of the cosmic-ray intensity
are closely related to the changes of pressure and temperature of the
atmosphere above the observer. While the pressure effect simply indicates
the dependence of cosmic radiation on the amount of air mass traversed,
the temperature effect has its origin in the instability of μ-mesons
(BPM38) which form the preponderant part of the penetrating component of
cosmic rays at sea level. The following simple argument shows qualitatively
that an increase of the temperature causes a decrease of the μ-meson in-
tensity at ground level. Each μ-meson produced at a certain atmospheric
depth - i.e., at a given pressure level - has to travel the distance from
the production layer to the ground in order to be detected. An increase
of the temperature will increase this distance, and thus enhance the pro-
bability of decay in flight. If all mesons were produced at the same at-
mospheric depth, and if one could neglect their ionization losses, the
fluctuations in the height, H, of a single pressure level - the production
level - would suffice to account for the temperature effect on the μ-meson
intensity. One could then express the variations of the integral μ-meson

---

* For a review, see, e.g., H. Elliot, Chapter VIII in "Progress in Cosmic
  Ray Physics" (North-Holland Publishing Company, 1952).

intensity, I, with an equation of the following type:

$$\delta I/I = A'_H \, \delta H + A'_P \, \delta x_o \tag{1}$$

where δH and δx_o are the variations of the height of production and of the ground pressure, respectively. The coefficients A'_H and A'_P are often referred to as the "decay" and "absorption" coefficients, respectively.

Early investigations seemed to confirm the approximate validity of the above regression formula. A. Duperier (DA44, DA48) in particular, found, through the statistical analysis of the observed data, that the ground pressure and the height corresponding to the atmospheric depth of 100 g cm^{-2} were the controlling factors in the variations of cosmic-ray intensity at sea level. However, the more recent studies by the same author (DA49), as well as those by D.W.H. Dolbear and H. Elliot (DDW51), have shown that the two-term equation (1) is inadequate to account fully for the variations of the cosmic-ray intensity at sea level. The inconsistencies have not been explained quantitatively in a satisfactory manner.

In what follows, we shall attempt to give a more rigorous, quantitative treatment of the problem outlined above. In particular, by making use of the intensity equation (II-8) we shall be able to take into account two facts customarily neglected in rough estimates of atmospheric effects: (1) the fact that the μ-mesons are produced continuously throughout the atmosphere, and (2) the fact that the μ-mesons suffer ionization losses during their propagation through air. As we shall see in the following sections, the first fact will justify and clarify the notion of an average production layer for the bulk of μ-mesons, and the second fact will introduce a third term into the regression formula discussed above. This additional term will turn out to be primarily controlled by the temperature changes in the lower atmosphere, where the ionization losses are relatively more important than in the upper atmosphere.

All considerations in this part apply only to the vertical intensities (both differential and integral) of μ-mesons measured at locations near sea level.

B. Temperature Effects on μ-Meson Intensity.

Let us discuss first the case where the ground pressure, x_o, is kept __constant__. Then the variation of $i_v(R,x_o)$ due to the temperature changes, $\delta T(x')$, is given, according to Eq. (II-8) by:

$$\delta_T i_v(R,x_o) = \int_0^{x_o} (\delta_T w/w)\, \oint (x,x_o,R)dx, \tag{2}$$

where

$$\oint(x,x_o,R) = G(R+x_o-x)e^{-x/L} w(x,x_o,R), \tag{2'}$$

and, according to Eq. (II-18),

$$\delta_T w/w = \alpha_H(x_o,R)\, \delta H(x,x_o) + \alpha_K(x_o,R)\, \delta K(x,x_o,R), \tag{3}$$

$$\delta H(x,x_o) = \frac{\mathcal{R}}{Mg} \int_x^{x_o} \frac{\delta T(x')}{x'}dx', \tag{4}$$

$$\delta K(x,x_o,R) = (x_o+R+b) \int_x^{x_o} \frac{\delta T(x')}{x_o+R+b-x'}\, dx' . \tag{4'}$$

In order to evaluate Eq. (2) we shall make use of the mean value theorem discussed in detail in the Appendix.

Evidently, the function $\oint$, defined by Eq. (2'), satisfies the condition (2) of the Appendix very well for $R > 100$ g cm^{-2}; furthermore, according to Eq. (II-22), the function δK satisfies the condition (1). Hence, we may apply the mean value theorem directly to the second term in Eq. (2). We cannot apply it directly to the first term, because the function δH displays a logarithmic divergence at $x = 0$. However, if we consider separately the bounded functions $\delta H/\ln(x_o/x)$ and $\oint \ln(x_o/x)$, rather than the functions δH and $\oint$, we readily verify that these two

functions do satisfy conditions (1) and (2), respectively. Consequently, we may write Eq. (2) as follows:

$$\delta_{T} i_{v}(R,x_{o}) = \frac{\alpha_{H}(x_{o},R)\,\delta H(x_{1},x_{o})}{\ln(x_{o}/x_{1})} \int_{0}^{x_{o}} \ln(\frac{x_{o}}{x})\,\bar{\Phi}\,dx$$

(5)

$$+ \alpha_{K}(x_{o},R)\,\delta K(x_{2},x_{o},R) \int_{0}^{x_{o}} \bar{\Phi}\,dx,$$

or

$$\delta_{T} i_{v}/i_{v} = \eta\,\alpha_{H}(x_{o},R)\,\delta H(x_{1},x_{o}) + \alpha_{K}(x_{o},R)\,\delta K(x_{2},x_{o},R),$$

(6)

where, according to Eq. (A-2),

$$x_{1} = \int_{0}^{x_{o}} x\ln(\frac{x_{o}}{x})\bar{\Phi}\,dx \bigg/ \int_{0}^{x_{o}} \ln(\frac{x_{o}}{x})\bar{\Phi}\,dx,$$

(7)

$$x_{2} = \int_{0}^{x_{o}} x\,\bar{\Phi}\,dx \bigg/ \int_{0}^{x_{o}} \bar{\Phi}\,dx,$$

(8)

and

$$\eta = \int_{0}^{x_{o}} \ln(\frac{x_{o}}{x})\,dx \bigg/ \left[\ln(\frac{x_{o}}{x_{1}}) \int_{0}^{x_{o}} \bar{\Phi}\,dx\right].$$

(9)

The three quantities, x_{1}, x_{2}, and η, according to their definitions, are functions of the residual range of μ-mesons at x_{o}, R. Figures 10 and 11 show these quantities plotted <u>versus</u> $R(100 < R < 4,000$ g cm$^{-2})$ for $x_{o} = 1,000$ g cm^{-2}. The calculations were carried out numerically whereas the function $\bar{\Phi}(x,x_{o},R)$ was computed with the aid of Eqs. (II-33) and (II-18)

Figure 10

Characteristic atmospheric depths $x_1(R)$ and $x_2(R)$ entering into the regression formula for the temperature effect on the differential μ-meson intensity near sea level, Eq. (III-6).

Figure 11

The quantity $\eta^{(R)}$ defined by Eq. (III-9) and entering into the regression formula for the temperature effect on the differential μ-meson intensity near sea level.
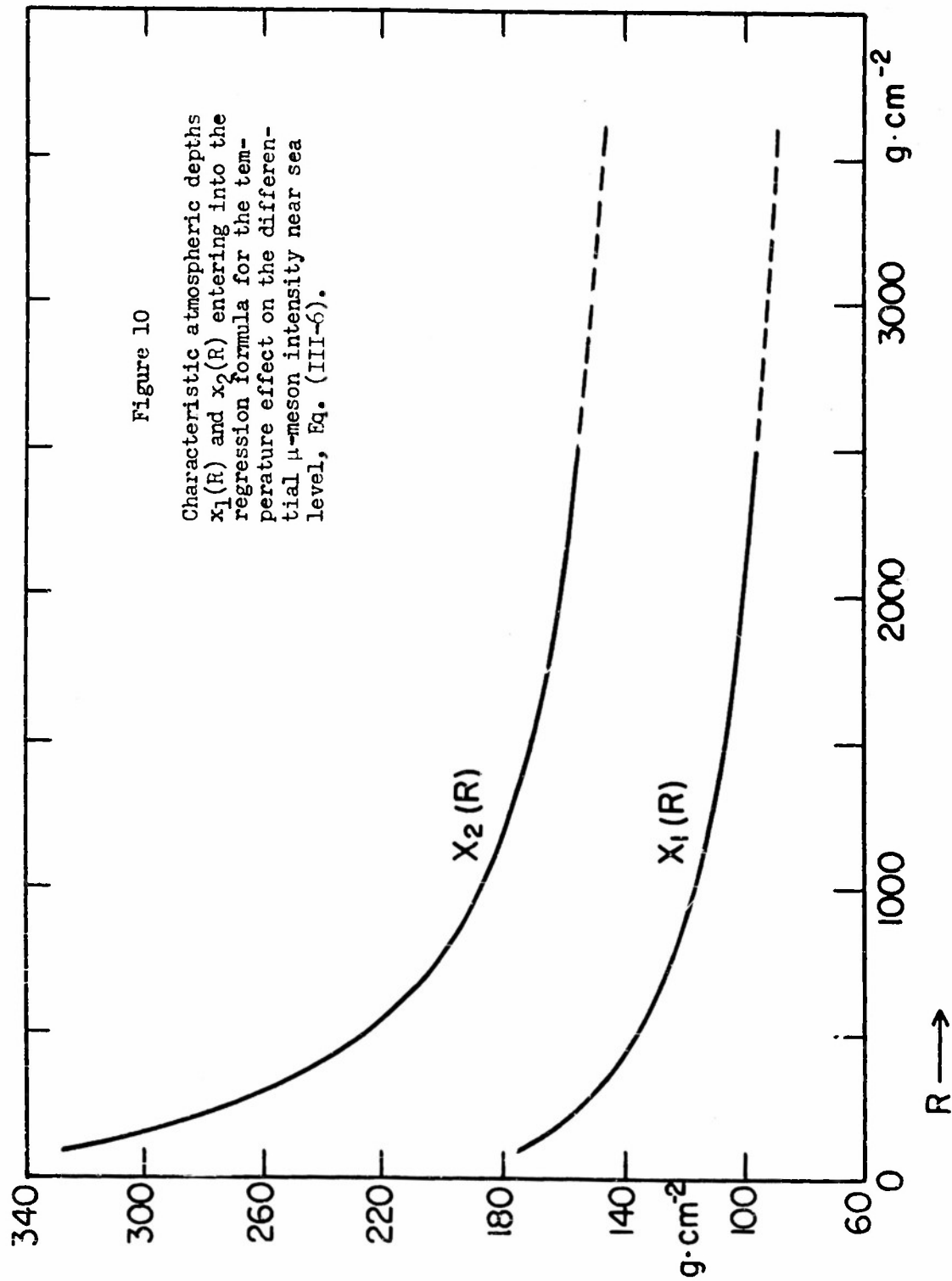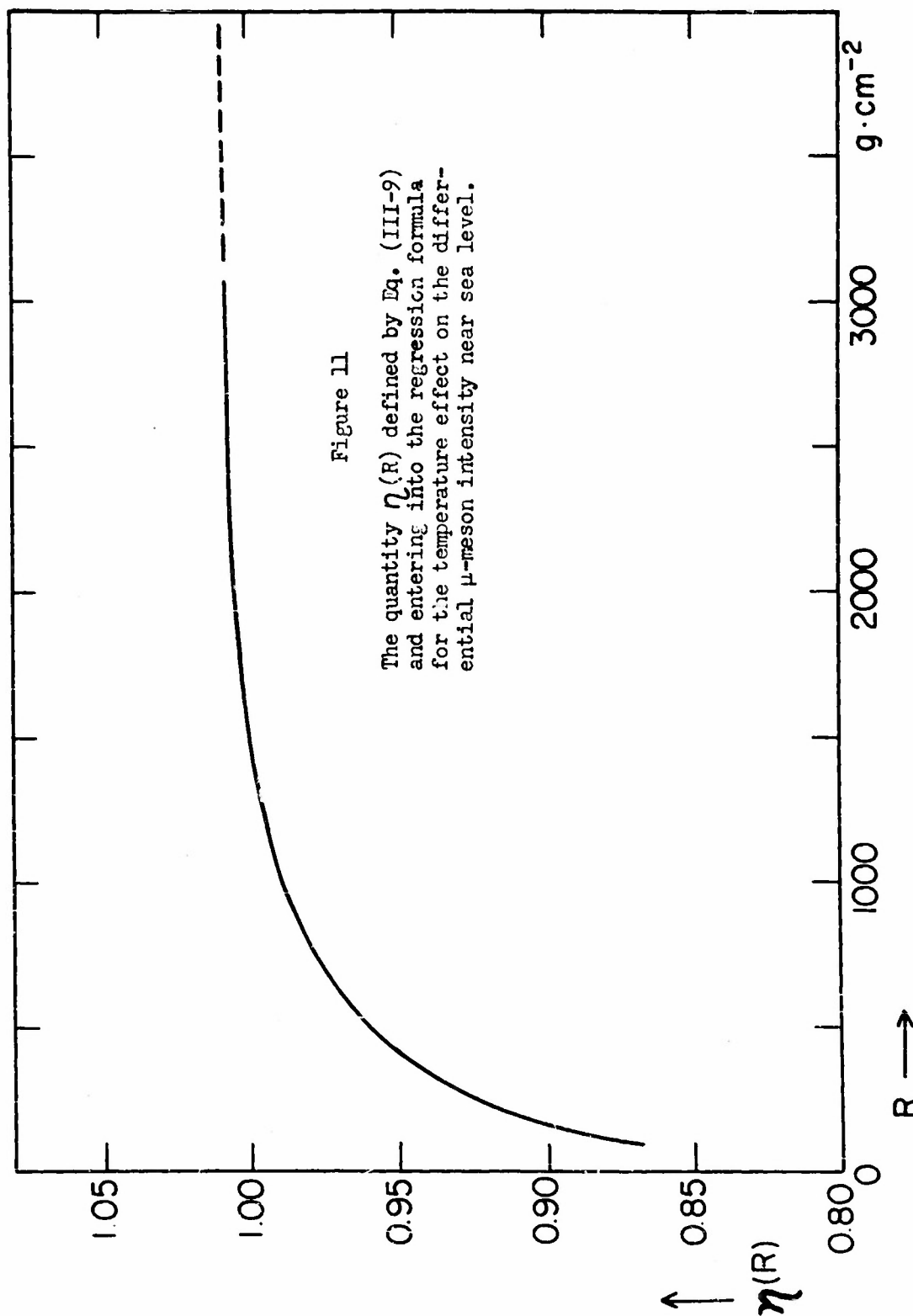
which corresponds to $40°$ of geographic latitude. Note that the factor η is practically one for all $R > 500$ g cm^{-2}; note further that the atmospheric depths x_1 and x_2 are slowly decreasing functions of R. We shall discuss the physical significance of these results in Section II-D.

In order to give Eq. (6) a simpler physical interpretation, it is useful to approximate the function δK by the following expressions:

$$\delta K(x_2,x_o,R) \approx \frac{x_o+R+b}{x_o-x_2} \ln\left(\frac{x_o+R+b-x_2}{R+b}\right) \int_{x_2}^{x_o} \delta T(x')dx' ;$$

one may readily verify that the above formula is a good approximation to Eq. (4) if $T(x')$ does not vary too strongly with x' in the region between x_o and x_2. In this case Eq. (6) simplifies to:

$$\delta_T i_v/i_v = a_H \delta H(x_1,x_o) + a_K (\delta T)_{AV}(x_2,x_o) , \tag{10}$$

where

$$
\left.
\begin{aligned}
a_H &= \alpha_H(x_o,R)\,\eta , \\[2mm]
a_K &= \alpha_K(x_o,R)\,(x_o+R+b) \ln\left(\frac{x_o+R+b-x_2}{R+b}\right) , \\[2mm]
(\delta T)_{AV}(x_2,x_o) &= \frac{1}{x_o-x_2} \int_{x_2}^{x_o} \delta T(x')dx' .
\end{aligned}
\right\} \tag{11}
$$

Eq. (10), although not so accurate as Eq. (6), gives us an insight into the problem in question: the temperature effect on the differential intensity, i_v, at sea level can be described by means of a two-term regression formula. The variations of i_v are to be correlated with the variations of the height of x_1 and the variations of the temperature averaged between x_2 and x_o. Figures 12 and 13 show the coefficients a_H and a_K plotted versus the residual ranges R.

Figure 12

The coefficients a_H and A_H correlating the differential and integral intensity changes with the variations of the mean production height; a_H and A_H are plotted versus R and R_o, respectively.

Figure 13

The coefficients a_K and A_K correlating the differential and integral intensity changes with the variations of the mean temperature of the troposphere; a_K and A_K are plotted versus R and R_o, respectively.

We conclude this section with a few remarks concerning the temperature effect for the integral intensity near sea level, I_v. Evidently, one obtains an expression applicable to this effect by integrating Eq. (6) or Eq. (10) over all residual ranges R above certain cut-off value, R_o, determined by the experimental arrangement, viz:

$$\delta_T I_v(R_o, x_o) = \int_{R_o}^{\infty} a_H i_v \delta H dR + \int_{R_o}^{\infty} a_K i_v (\delta T)_{Av} dR . \qquad (12)$$

Since the functions δH and $(\delta T)_{Av}$ vary very slowly with respect to R, Eq. (12) may be evaluated by means of the mean value theorem. Thus, according to Eqs. (A-1') and (A-2):

$$\delta_T I_v / I_v = A_H \delta H(\bar{x}_1, x_o) + A_K (\delta T)_{Av}(\bar{x}_2, x_o) , \qquad (12')$$

where

$$A_{H,K} = \frac{1}{I_v} \int_{R_o}^{\infty} a_{H,K} i_v dR ;$$

$$\bar{x}_1 = x_1(R_1) , \quad \bar{x}_2 = x_2(R_2) ; \qquad (13)$$

$$R_{1,2} = \int_{R_o}^{\infty} R a_{H,K} i_v dR \bigg/ \int_{R_o}^{\infty} a_{H,K} i_v dR.$$

Figures 12 and 13 show the coefficients A_H and A_K plotted against the cut-off range, R_o. These curves are convenient for comparative purposes with experimental observations. We shall return to them in Section II-D.

The numerical values of $\bar{x}_1$ and $\bar{x}_2$ for the case of $I_v(R_o)$ may be estimated directly from Figure 10 where one has to take those values of x_1 and x_2 which correspond to the average residual ranges R_1 and R_2,

respectively. One finds that $\bar{x}_1$ will lie somewhere between 115 and 110 g cm^{-2}, and $\bar{x}_2$ between 190 and 160 g cm^{-2}, depending on the experimental value of R_o.

C. Pressure Effect on μ-Meson Intensity.

To complete the discussion of the atmospheric effects on the cosmic-ray intensity it remains to evaluate the effect of the atmospheric pressure. This evaluation may be carried out by a method analogous to that discussed in the preceding section. If the temperature overhead is kept constant, the partial variation of the differential intensity, $i_v(R,x_o)$, due to the changes of the ground pressure, x_o, is given by:

$$\delta_P i_v(R,x_o) = \frac{\partial i_v(R,x_o)}{\partial x_o}\ \delta x_o \ . \tag{14}$$

Assuming that i_v may be represented by Eq. (II-8) one finds by differentiation:

$$\delta_P i_v = \left\{ G(R)e^{-x_o/L} + \int_0^{x_o} \frac{\partial}{\partial x_o}\Big[\ln G(R') + \ln w(x,x_o,R)\Big]\Phi\ dx \right\}\delta x_o \ . \tag{14'}$$

The first term in Eq. (14') is negligible at sea level. The two last terms may be evaluated by means of the mean value theorem discussed in the Appendix. By substituting Eqs. (II-33) and (II-18) for $G(R')$ and $w(x,x_o,R)$, respectively, one gets:

$$\delta_P i_v / i_v = a_P \delta x_o \ , \tag{15}$$

where the "pressure" coefficient, a_P, is given by:

$$a_P = - \frac{3.58}{520 + x_o + R - x_2} + \eta \frac{\partial \alpha_H(x_o,R)}{\partial x_o}\ H(x_1,x_o)$$

$$+ \alpha_H(x_o,R)\frac{\mathscr{R}T(x_o)}{\bar{M}gx_o} + \frac{\partial}{\partial x_o}\Big[\alpha_K(x_o,R)\ K(x_2,x_o,R)\Big] \ . \tag{16}$$

The evaluation of Eq. (16) with the help of Eqs. (II-19) to (II-22) and Fig. 6 shows that the first term above is prominent. We have computed

the pressure coefficient a_p for $100 < R < 4,000$ g cm^{-2} by using for the temperature, $T(x)$, the annual average at 40° N geographic latitude. The result is presented in Fig. 14, where a_p is plotted versus R.

For the convenience of the reader we have also computed the pressure coefficient of the integral intensity, i.e., the quantity:

$$A_P = \frac{1}{I_v} \int_{R_o}^{\infty} a_p i_v dR .$$ (17)

The behavior of A_p, as a function of R_o, is shown in Fig. 14.

Before concluding this section, we should like to point out that the coefficient a_p is directly related to the measurements on the altitude dependence of the differential intensity, i_v: according to its definition a_p simply represents the slope of the intensity-depth curve. Therefore, referring to Eq. (16), the observed values of a_p may be alternately used to check the correctness of the logarithmic derivative of $G(R')$.

D. Summary. Comparison with Experiments.

(a) Atmospheric effect on the differential intensity.

According to the results obtained in Sections B and C the total variation of the differential intensity near sea level may be represented by a three-term regression formula, viz:

$$\delta i_v / i_v = a_H \delta H(x_1, x_o) + a_K (\delta T)_{Av}(x_2, x_o) + a_P \delta x_o ,$$ (18)

i.e., the fractional changes in i_v are to be correlated with the following variables of the atmosphere:

    1) the departure from the mean height, δH, of the pressure $x_1(R)$;

    2) the departures from the mean temperature overhead averaged between the pressure level $x_2(R)$ and the sea-level pressure, x_o, viz:

$$(\delta T)_{Av}(x_2, x_o) = \frac{1}{x_o - x_2} \int_{x_2}^{x_o} \delta T(x') dx' ;$$

Figure 14

The coefficients a_p and A_p correlating the differential and integral intensity changes with the variations of the sea-level pressure; a_p and A_p are plotted versus R and R_o, respectively.
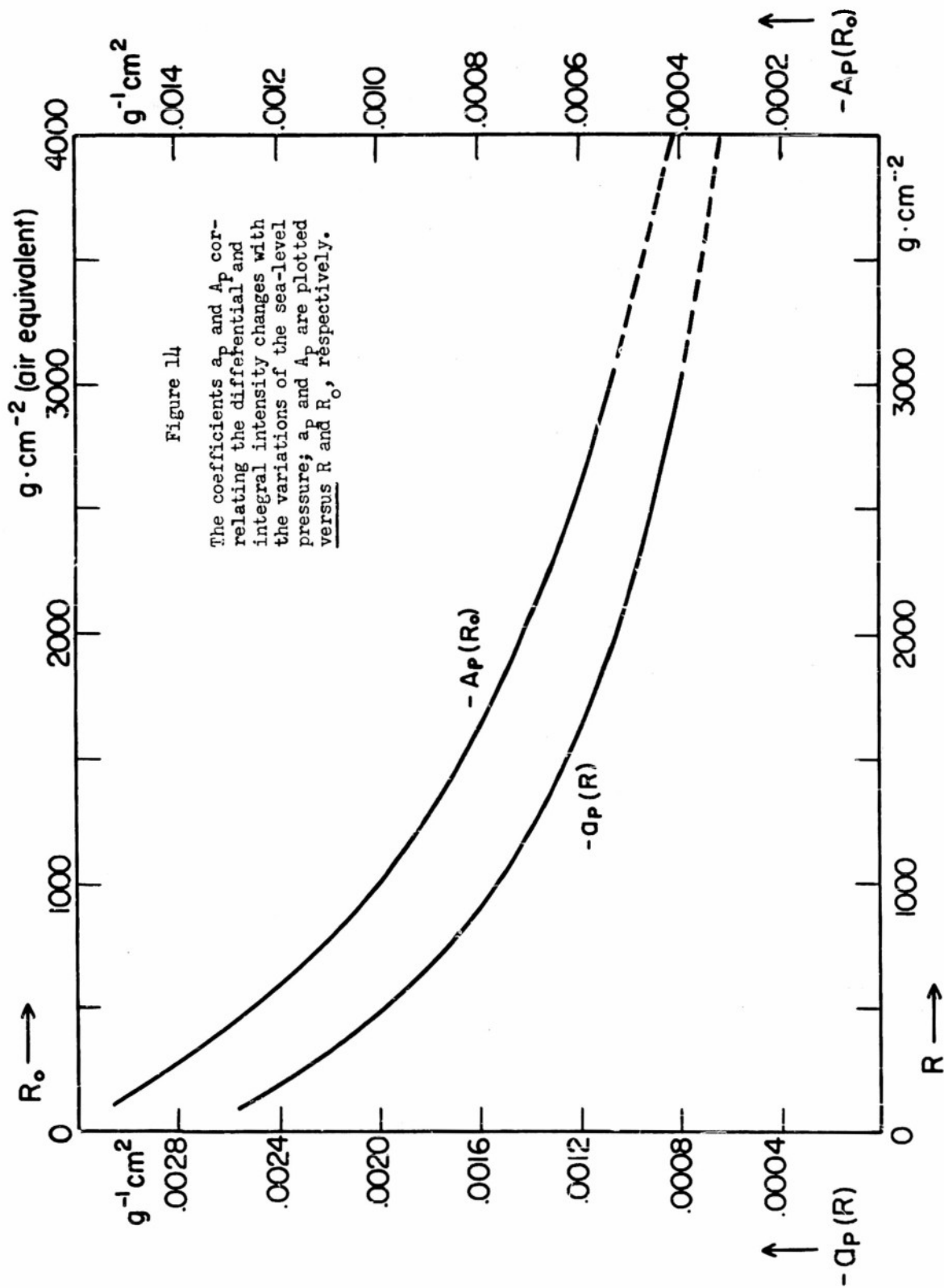
3) the departure from the mean pressure at sea level, δx_o.
The numerical values of the two characteristic pressure levels, x_1 and x_2,
are to be taken from Fig. 10. For the numerical values of the three co-
efficients, a_H, a_K, and a_P, one is referred to the Figures 12, 13 and 14.

(b) Atmospheric effect on the integral intensity.

Similarly to case (a), the total variation of the integral intensity
near sea level is given by:

$$\delta I_v/I_v = A_H \delta H(\bar{x}_1, x_o) + A_K(\delta T)_{Av}(\bar{x}_2, x_o) + A_P \delta x_o. \qquad (19)$$

Here the coefficients A_H, A_K, and A_P are constant quantities for a given
experimental arrangement. Their numerical values will be, however, dif-
ferent from case to case, depending on the amount of shielding material
above the detector. Taking 400 g cm^{-2} air equivalent of shielding material
as a typical case, we find from Figures 12, 13 and 14:

$$\left. \begin{array}{l} A_H = -3.15\% \text{ per km,} \\ A_K = -0.059\% \text{ per } {}^\circ C, \\ A_P = -1.79\% \text{ per cm Hg.} \end{array} \right\} \qquad (20)$$

In order to determine the above coefficients experimentally, one has
to correlate the observed changes in I_v with the three atmospheric
variables $\delta H(\bar{x}_1, x_o)$, $(\delta T)_{Av}(\bar{x}_2, x_o)$ and δx_o. The characteristic
pressure levels, $\bar{x}_1$ and $\bar{x}_2$, have now practically fixed values: $\bar{x}_1 \approx 115 \text{ g cm}^{-2}$,
and $\bar{x}_2 \approx 190 \text{ g cm}^{-2}$, if the amount of shielding above the detector is of
the order of a few hundred g cm^{-2}. It is worth mentioning that the pres-
sure level $\bar{x}_2$ nearly coincides with that of the tropopause at moderate
latitudes. This implies that the vertical average of the temperature
changes above the observer $(\delta T)_{Av}$, extends only over the region of the
troposphere, and does not include the temperature of the stratosphere.

(c) Comparison with experiments.

As we have mentioned in Sec. A, it has been customary to correlate
the observed variations of the μ-meson intensity with only two atmos-
pheric variables, δH and δx_o. Lack of knowledge of the third variable,

$(\delta T)_{Av}$, makes an exact comparison of our results with those found experimentally impossible. However, the following semi-quantitative considerations appear to indicate substantial agreement between observations and theory.

In the first place, our value of 115 g cm^{-2} for the "mean pressure level" of μ-meson production is in agreement with the observations. For example, we have already mentioned that A. Duperier obtained the best correlation between changes in cosmic-ray intensity and changes in the height of a given pressure level by choosing a value of this pressure level in the proximity of 100 g cm^{-2}.

In the second place, if one writes Eq. (19) in the form:

$$\delta I_v/I_v = \left[A_H + A_K \frac{(\delta T)_{Av}}{\delta H}\right]\delta H + A_P \delta x_o , \qquad (21)$$

one sees that the so-called "decay" coefficient of Eq. (1), A_H', is related to our coefficients A_H and A_K by the equation:

$$A_H' = A_H + A_K \frac{(\delta T)_{Av}}{\delta H} . \qquad (22)$$

The ratio $(\delta T)_{Av}/\delta H$ will depend, of course, on the geographic location, the season during which the experiment was performed, etc. Meteorological observations indicate that, for moderate latitudes, the above ratio will have on the average the following approximate values:

for diurnal departures of $(T)_{Av}$ and H from their means

$$\left[(\delta T)_{Av}/\delta H\right]_{diurnal} \approx 50 \quad (^{o}C/km),$$

for seasonal departures of $(T)_{Av}$ and H from their means

$$\left[(\delta T)_{Av}/\delta H\right]_{seasonal} \approx 20 \quad (^{o}C/km).$$

It follows that the decay coefficient, A_H', will be different depending on whether it is inferred from the diurnal on the seasonal changes of the intensity. According to Eqs. (20) and (22), one would expect for A_H' in these two cases:

$$\left[A_H'\right]_{diurnal} \approx -6.1 \text{ % per km},$$

$$\left[A_H'\right]_{seasonal} \approx -4.3 \text{ % per km}.$$

Indeed, the diurnal and seasonal decay coefficients estimated above are in substantial agreement with those observed experimentally. For instance, Dolbear and Elliot (DDW51) deduced for $A_H^!$ the values -5.7 % km^{-1} and -3.6 % km^{-1} from the daily and monthly correlations, respectively.[*]

Regarding the pressure effect on the μ-meson intensity, we shall limit ourselves to the remark that the values of the pressure coefficients a_P and A_P, given in Fig. 14, seem to be in essential agreement with those observed experimentally. This can be demonstrated by a comparison of the differential range spectra for two different depths near sea level, as, e.g., the spectra measured by Conversi in Chicago (1,010 g cm^{-2}) and at China Lake (957 g cm^{-2}). One finds that by correcting the sea-level spectrum given in Fig. 2 by means of a_P for the two corresponding levels one obtains two curves practically identical with those given by Conversi (CM50). The agreement may be considered as a partial check for the correctness of the production spectrum of μ-mesons.

In conclusion, we would like to discuss briefly the problem of the so-called "positive temperature effect". As we have mentioned in Sec. A recent observations by Duperier have shown that the two-term regression formula given by Eq. (1) was inadequate to account fully for the observed variation of the cosmic-ray intensity. The analysis of the correlation coefficients indicated that there must be an additional atmospheric variable which, together with H and x_e, plays a controlling role in the intensity variations. Duperier assumed this variable to be the temperature of the pressure layer between 100 and 200 mb (lower stratosphere). Hence, he replaced Eq. (1) by the following:

$$\delta I/I = A_H \delta H + A_T \delta T + A_P \delta x_0 , \qquad (23)$$

where δT is the deviation from the mean of the temperature of the 100-200 mb pressure layer, and the other symbols have the same meaning as before. The temperature coefficient, A_T, deduced from the observational

---

[*] In the experimental arrangement used by Dolbear and Elliot the threefold counter coincidence set was inclined at 45° to the vertical. Therefore, the results of these authors are to be corrected before being compared with the results corresponding to the vertical intensity. It can be shown, however, that this correction is not crucial, and can be neglected in our semi-quantitative discussion.

data, turned out to be positive (A_T = 0.12 % per ^{o}C). Duperier attempted to interpret this positive temperature effect as due to the competing processes of nuclear capture and decay of π-mesons. However, a quantitative estimate of the effect of these processes, based on more recent data for the mean life and the cross section for nuclear capture of π-mesons, shows that the observed value of A_T is much too high to be ascribed exclusively to the finite life span of π-mesons.

It is interesting to compare Duperier's regression formula, Eq. (23), with that given by Eq. (19). Since the coefficients A_H and A_P determined by Duperier are roughly in numerical agreement with those calculated in this paper, the ratio $(\delta T)_{Av} / \delta T$ should be equal to A_T/A_K. The value of our coefficient, A_K, is about -0.06 % per ^{o}C while the experimental value of A_T is 0.12 % per ^{o}C from which it follows that $(\delta T)_{Av} / \delta T \approx$ -2. The negative sign of the ratio $(\delta T)_{Av} / \delta T$ is not in contradiction with the general behavior of the free atmosphere. For it is well known that the warming up of the troposphere $[(\delta T)_{Av}$ positive] is, as a rule, accompanied by a cooling down of the lower stratosphere (δT negative) and vice versa. The magnitude of the above ratio is probably too large. However, a knowledge of the actual values of $(\delta T)_{Av}$ for the period and location of Duperier's experiment is needed to check our results quantitatively.

In view of the above discussion we conclude that the additional term, $A_K(\delta T)_{Av}$, in the regression formula may well remove the apparent seasonal variability of Elliot's decay coefficient as well as the anomalous value of Duperier's coefficient for the positive temperature effect. An experimental verification of this conclusion would be desirable. Unfortunately, because of the strong correlation between δH and $(\delta T)_{Av}$, it will be very difficult to separate experimentally the effects caused by δH from those caused by $(\delta T)_{Av}$.

IV. LATITUDE DEPENDENCE OF μ-MESON SPECTRUM AT PRODUCTION

A. Introductory Remarks.

Ever since the earliest years of cosmic-ray research it has been known that the local charged cosmic radiation changes in a definite pattern when one passes from south to north on our globe (for a review, see, for example, NHV52). This empirical evidence, although not understood in all

detail, has had a great heuristic value in guiding physicists toward a more fundamental phenomenon: the geomagnetic effect on the primary cosmic radiation. Today we are in a position to link the predicted effects of the earth's magnetic field with those observed experimentally and thus to strive for a consistent picture of all phenomena related to the latitude variation of cosmic rays. Among several striking features concerning the behavior of a charged particle in the earth's magnetic dipole, the following will be of particular interest to us: a charged particle of energy lower than a certain limit is prevented from reaching the top of our atmosphere and thus is excluded in the observed energy spectrum of the primary radiation. The value of this cut-off energy depends on the charge and mass of the particle, and changes with geomagnetic latitude as well as with the angle of incidence. Columns 2 and 3 of Table II show these values for the case of vertical protons and α-particles (predominant constituents of primary radiation). The observations at high altitudes carried out by means of rockets and balloons not only support the theoretical predictions on the cut-off effect but also provide us with the absolute numbers of primary particles which reach the upper atmosphere at various geomagnetic latitudes. The results obtained by Winckler et al. (WJR50) are compiled in column 4 of Table II.

Since we are concerned with the analysis of the meson component of the cosmic radiation, the problem which is of importance to us is the following: how does the latitude variation of the primary flux affect the production of π-mesons and thus the production spectrum of μ-mesons? Qualitatively, it is evident that the observed decrease in the primary flux should lead to a reduction of the number of π-mesons produced. (The above statement would be untrue only if primary particles of energies below the cut-off limits at the geomagnetic equator were completely inefficient in meson production.) However, in order to estimate quantitatively the magnitude of this reduction on the basis of the observed decrease of the primary radiation, one would have to know the cross sections for the production of π-mesons as functions of the energy of primary particles. Since, for the energy region with which we are concerned here, the cross sections are not known, the only way to obtain some information c the latitude dependence of the μ-meson spectrum at production is to study the latitude

TABLE II

Geomagnetic data pertinent to the primary radiation and the π- and μ-meson components. The symbols below have the following meaning: φ is the geomagnetic latitude; E_p and E_α are the kinetic cut-off energies of vertical primary protons and α-particles, respectively; j is the total vertical intensity of primary radiation (WJR50); $r'_\varphi = \left[i_v(100,300)\right]_\varphi / \left[i_v(100,300)\right]_{50^o}$, where $i_v(100,300)$ is the differential vertical intensity of μ-mesons with the residual range of 100 g cm^{-2} at the atmospheric depth of 300 g cm^{-2}, for a given geomagnetic latitude, φ (CM50); a is the parameter appearing in the empirical formula for the production spectrum of μ-mesons: $G(R') = 7.31 \times 10^4 (a+R')^{-3.58}$, Π is the total number of π-mesons of energies greater than 260 Mev produced throughout the atmosphere in the downward cone.

φ	E_p Bev	E_α Bev	j cm^{-2}sec^{-1} sterad^{-1}	r'	a g cm^{-2}	Π cm^{-2}sec^{-1} sterad^{-1}
1	2	3	4	5	6	7
0°	14.6	27.2	0.026	0.55	646	0.135
10°	12.5	23.3	0.027	0.56	640	0.139
20°	10.1	18.6	0.031	0.60	627	0.145
30°	7.3	13.1	0.046	0.70	591	0.165
40°	4.3	7.1	0.080	0.87	546	0.197
50°	1.8	3.2	0.180	1.00	520	0.217
60°	0.43	0.53	0.290	1.04	513	0.225

dependence of measurable quantities which are related in a known fashion
to the μ-meson spectrum at production. One such quantity is the differential
vertical intensity of μ-mesons discussed already in the preceding sections;
its relation to the μ-meson spectrum at production is expressed by Eqs. (II-8),
(II-18) and (II-33). It follows from Eq. (II-8) that, from the known de-
pendence of $i_v(R,s)$ and $w(x,s,R)$ on geomagnetic (or geographic) latitude,
one should be capable of drawing some conclusions about the latitude de-
pendence of the μ-meson spectrum at production.

B. Experimental Evidence of Latitude Dependence of μ-Meson Intensity.

In contrast to the abundance of the experimental material concerning
the latitude dependence of the total penetrating cosmic radiation the in-
formation on the latitude dependence of the differential μ-meson intensity
itself is very incomplete. It is true that near sea level one can identify
the total penetrating cosmic radiation with the μ-meson component and thus
regard it as usable for our analysis. However, the latitude variation is
so greatly reduced near sea level as compared with higher elevations that
it does not represent any promising basis for quantitative estimates of
the latitude dependence of the meson spectrum at production. As far as
the high-altitude measurements are concerned, we know of only one experi-
ment, namely, that carried out by M. Conversi (CM50) aboard an aircraft
in several series of flights at various latitudes. Conversi's measure-
ments were made at the constant altitude of 30,000 feet with the apparatus
and technique discussed in Part II, Sec. B. Thus his data can be inter-
preted as a direct measure for the latitude dependence of $i_v(R,s)$ for
$R = 100$ g cm^{-2} and s = 307 g cm^{-2}. Unfortunately, the statistical accuracy
achieved in this series of measurements is poor (at some latitudes the
errors exceed 20 percent) so that not much weight can be given to the
shape of the latitude curve chosen by Conversi as the best fit to the
small numbers of points obtained. Nevertheless, it is well to remember
that this curve still represents the best information on the latitude de-
pendence of μ-meson intensity at high altitudes available at the present
time.

It will be useful for the purpose of our discussion to express the
μ-meson intensities measured at various latitudes in multiples of the in-
tensity at 50° N geomagnetic latitude rather than at the geomagnetic equa-
tor. Referring to Conversi's curve, we quote these ratios in column 5 of
Table II.

C. Atmospheric Latitude Effect.

It follows from the discussion sketched in Sec. A that there are actually two causes for the observed variation of the μ-meson intensity with latitude. While the first cause originates in the geomagnetic cut-off of the primary spectrum and affects the μ-meson spectrum at production, the second cause originates in the latitude dependence of the vertical distribution of the atmospheric temperature and affects the survival probability of μ-mesons. Although, as we shall see later, the latter effect proves to be in general of minor importance, in some special cases it cannot be disregarded completely. Thus, before attempting any quantitative deductions concerning the geomagnetic effect on the production spectrum, we must assure ourselves as to the magnitude of the second effect.

Let us first discuss in general terms how the existing temperature distribution in our atmosphere affects the intensities of μ-mesons. If we limit ourselves to the annual mean conditions on our globe we can base our considerations on Fig. 4. This figure implies that if we move south-wards along an isobaric surface below the tropopause we encounter in the northern hemisphere a positive temperature gradient. On the other hand, an excursion above the tropopause in the same direction is confronted, as a rule, by a temperature gradient of the opposite sign. Since, according to Eq. (II-18), an increase in values of the integrals $\int_x^s T(x')dx'/x'$ and $\int_x^s T(x')dx'$ reduces the chance of survival of a μ-meson, it follows that the existing horizontal temperature gradients can reduce or enhance the μ-meson intensities depending on whether we make the measurements (moving southward) below or above a certain atmospheric depth. The layer where this atmospheric latitude effect changes its sign is to be expected some-where between 250- and 300-mb levels. As to the magnitude of the effect, we infer further from Fig. 4 that its absolute value is greatest for the intensity measurements near sea level.

All the above findings are confirmed by explicit numerical calculations. For observations near sea level we can apply the regression formula (III-10) to estimate the relative changes of μ-meson intensities with respect to that at $40°$ geographic latitude. The results of our calculations are shown in the first 6 columns of Table III. One notes that, whereas for high-energy mesons the effect amounts only to a few percent, the relative change of

TABLE III

Atmospheric latitude effect on the μ-meson intensity near sea level and at the depth of 300 g cm^{-2}. The symbols $\left[\delta i_v / i_v\right]_{\varphi'}$ represent the relative departures of the $i_v(R,s)$-values at a given geographic latitude, φ', from the corresponding $i_v(R,s)$-values at $40°$ geographic latitude.

φ'	$\left[\delta i_v(R,x_o)/i_v(R,x_o)\right]_{\varphi'}$					$\left[\dfrac{\delta i_v(100,300)}{i_v(100,300)}\right]_{\varphi'}$
	$R = 100$ g cm^{-2}	500	1,000	1,500	2,000	
$0°$	-0.0670	-0.0341	-0.0196	-0.0132	-0.0093	-0.0164
$30°$	-0.0309	-0.0155	-0.0089	-0.0059	-0.0042	-0.0055
$40°$	0	0	0	0	0	0
$50°$	0.0324	0.0156	0.0087	0.0056	0.0038	0.0057
$60°$	0.0553	0.0283	0.0170	0.0119	0.0088	0.0145

slow-meson intensities can be considerable. They are certainly not negligible if one compares the differential intensities of μ-mesons with R = 100 g cm^{-2} observed at middle latitudes with those observed near the equator.

Regarding the atmospheric latitude effect at high elevations we are particularly interested in the quantitative estimate of $\left[\delta i_v / i_v\right]_p$, at s = 300 g cm^{-2} and R = 100 g cm^{-2} (Conversi's measurements). Since for this atmospheric depth the regression formula (III-10) is not applicable [see condition (2) in the Appendix] we have carried out rigorous numerical computations of $i_v(100, 300)$ for various geographic latitudes by making use of Eq. (II-8) and Fig. 4. The results expressed in terms of relative departures from the $i_v(100, 300)$-values at 40° geographic latitude are given in the last column of Table III. One sees that the effect is small, as expected from the above qualitative considerations.

Before closing this section we would like to clarify one point: in our numerical calculations we have tacitly assumed that the production spectrum G(R'), is identical at all latitudes and is given by Eq. (II-33). Although this assumption as such is certainly wrong, it can be shown that the quantities quoted in Table III are practically unaffected by the variation of G(R'). Consider, for instance, the sea-level data computed on the basis of Eq. (III-10). Among the quantities appearing on the right-hand side of this latter equation, only η, x_1, and x_2 are affected by the assumed values of G(R'). If one takes into account their insensitivity with respect to G(R'), and the manner in which they enter Eq. (III-10), one concludes that the relative intensity changes caused by horizontal temperature gradients at constant pressure are practically independent of the actual variations of the production spectrum.

D. Geomagnetic Effect on the μ-Meson Spectrum at Production.

The discussion of the foregoing sections indicates that there are several advantages which are offered by the study of the latitude dependence of μ-meson intensities at high altitudes. Among others, the following are worth mentioning: (1) the effect is sufficiently large to be recognized as real even with considerable statistical and instrumental errors: (2) the atmospheric latitude effect is insignificant. In other words, the latitude dependence of μ-meson intensity in the proximity of 300 mb originates

almost exclusively from the geomagnetic effect on the μ-meson spectrum
at production. We may, therefore, use Conversi's latitude curve as a
direct index for the latitude variations of this quantity. Although it
is evident that Conversi's curve alone is not sufficient to determine
completely the behavior of $G(R')$ at all latitudes, it can be of great
value if it is supplemented by some additional information. One such
information is the fact that at large residual ranges the production
spectrum is nearly independent of the geomagnetic latitude. This follows
from the nature of the geomagnetic effect. A μ-meson with a residual
range larger than, say, $3,000$ g cm^{-2} has for its parent a π-meson of
kinetic energy of not less than 8 Bev (see Fig. 16). A π-meson of
that high energy can be produced by the primary particle only if the
energy of the latter exceeds 12 Bev. Thus, most of the μ-mesons with
residual ranges above $3,000$ g cm^{-2} are originated by primaries which
are sufficiently energetic to overcome the magnetic field of the earth
at all latitudes. Hence, the production spectrum of μ-mesons shown in
Fig. 8 ($3,000$ g cm$^{-2} < R' < 7.000$ g cm^{-2}) represent a solution not only
for 50° geomagnetic latitude but for all latitudes.

Let us make a tentative assumption that the production spectrum,
$G(R')$, can be expressed at all latitudes by a formula of the type given
by Eq. (II-32). Then we see that among the three characteristic con-
stants, C, a and γ, only a can depend on the geomagnetic latitude as a
is the only constant with respect to which $G(R')$ is insensitive at large
ranges. Expressing this in symbols we expect $G(R')$ to be given by:

$$G(R') = \frac{7.31 \times 10^{4}}{\left[a(\varphi)+R'\right]^{3.58}} \left[g^{-2}cm^{2}sec^{-1}sterad^{-1}\right], \quad (1)$$

where φ indicates the geomagnetic latitude. The determination of the
latitude dependence of $a(\varphi)$ represents a relatively simple problem.
By computing the right-hand side of Eq. (II-8) for various values of
$a(\varphi)$ at constant R and s and by comparing the results with the $i_v(R,s)$ -
values pertinent to given geomagnetic latitude, $\left[i_v(R,s)\right]_{\varphi}$, one arrives
at the functional relation between $a(\varphi)$ and $\left[i_v(R,s)\right]_{\varphi}$. Referring to
Conversi's latitude curve we show in Fig. 15 the functional relation between

Figure 15

Latitude dependence of the constant a occurring in the empirical formula for the production spectrum of μ-mesons, viz.; $G(R') = 7.31 \times 10^4 \, (a+R')^{-3.58}$. The constant a is plotted versus the intensity of μ-mesons with the residual range of 100 g cm^{-2} at the depth of 300 g cm^{-2} measured at given geomagnetic latitude and expressed in multiples of the corresponding intensity at 50° geomagnetic latitude.
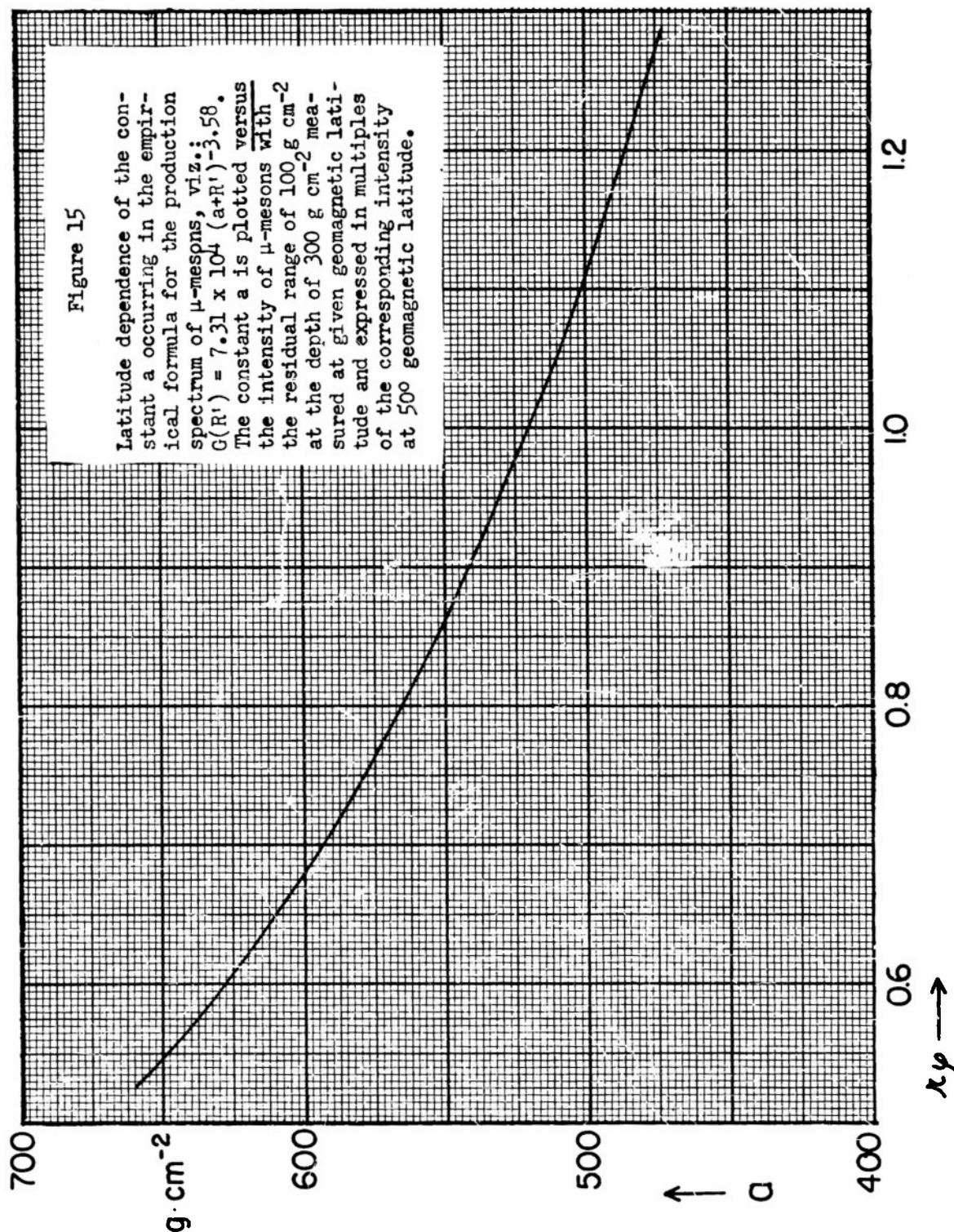
$a(\varphi)$ and r_φ where r_φ is the ratio of $\left[i_v(100, 300)\right]_\varphi$ to $\left[i_v(100, 300)\right]_{50°}$, corrected for the atmospheric latitude effect (see column 6 in Table III). With the help of this figure and column 5 of Table II one then finds $a(\varphi)$ as a function of φ (see column 6 in Table II). One notes that $a(\varphi)$ varies from 646 g cm^{-2} at the geomagnetic equator to 513 g cm^{-2} at $60°$ geomagnetic latitude. Among all these values of a, the value of 520 g cm^{-2} at $50°$ geomagnetic latitude is to be considered as most reliable. Its correctness has been verified in Part II where we had at our disposal a relatively accurate and complete set of experimental data.

It is desirable to test how plausible is our assumption that $G(R')$ may be expressed at all latitudes by Eq. (1). This can be done, for example, by comparing the i_v-values observed at depths s different from 300 g cm^{-2} and latitudes φ different from $50°$ with corresponding i_v-values computed on the basis of Eqs. (1) and (II-8). L. del Rossario and J. Dávila-Aponte (RL52) have measured the range spectrum of slow mesons at sea level at $29°$ N geomagnetic latitude. They found that $i_v(100,x_0)=(4.25 \pm 0.13) \times 10^{-6}$(g-sec-sterad)$^{-1}$. Our calculations for the same latitude $a(29°) = 595$ g cm^{-2} yielded, after the correction for the atmospheric latitude effect, $i_v(100,x_0) = 4.17 \times 10^{-6}$(g-sec-steard)$^{-1}$.

V. PRODUCTION SPECTRUM OF π-MESONS

A. Significance of π-Meson Spectrum.

The topics discussed thus far have emphasized primarily the "practical" usefulness of the μ-meson spectrum at production, $G(R')$. With the aid of $G(R')$ we were able to predict the numerical values of quantities which could be measured directly by existing experimental techniques. Now we turn to considerations which point in a different direction. With the aid of $G(R')$ we shall attempt to derive a quantity which is not accessible to present cosmic-ray experiment but has a direct physical meaning; this quantity is the energy spectrum of charged π-mesons at production. Its importance stems from several reasons. To mention a few, the knowledge of the energy spectrum of charged π-mesons throws more light upon the properties of high-energy nuclear interactions; by analogy arguments it leads to the production spectrum of neutral π-mesons and, thus, to the

source function for the electronic component. These problems are actually beyond the scope of this analysis. We should like, however, to touch at least upon one topic: the multiplicity problem of π-meson production from nuclear interactions in the energy region of several Bev.

B. Evaluation of Energy Spectrum of π-Mesons from the Range Spectrum of μ-Mesons at Production.

Owing to the experimental evidence that the π-meson decay is a two-body process $(\pi^{\pm} \rightarrow \mu^{\pm} + \nu)$ we can derive a relation between the energy spectrum of the μ-meson at decay, $P(U_\pi)$, and the energy spectrum of μ-mesons at production, $M(U)$. We have quoted this relation already in Part II, Sec. B, Eq. (II-3). Since in our case $P(U_\pi)$ is the unknown quantity, it is desirable to solve Eq. (II-3) with respect to $P(U_\pi)$. According to Ascoli (AG50) this solution can be represented in terms of the following infinite series:

$$P(U_\pi) = D(U_1) + D(U_2) + \ldots , \tag{1}$$

where

$$D(U) = -\left(\frac{m_\pi}{m_\mu} - \frac{m_\mu}{m_\pi}\right) \frac{dM(U)}{dU} \sqrt{U^2 - 1} , \tag{2}$$

and U_1, U_2, U_3 ... is a sequence of μ-meson energies uniquely determined by the π-meson energy U_π. The numerical values of U_1, U_2, U_3 ... can be obtained from Fig. 16 by the following procedure:

Beginning with a vertical line corresponding to a given value of U_π, find U_1 which represents the highest energy of a μ-meson born from a π-meson of energy U_π. Proceeding from this point with straight lines, alternately horizontal and vertical, inscribe a step curve within the smooth curve drawn in Fig. 16. The points obtained on the upper branch of the smooth curve then represent, in increasing order, the required sequence U_1, U_2, U_3 ...

In order to obtain an explicit expression for Eq. (2) we recall that, according to Eq. (II-5), $M(U) = G(R')/k(U)$; thus:

$$\frac{dM(U)}{dU} = -\frac{1}{k^2(U)} \left[G(R') \frac{dk(U)}{dU} - \frac{dG(R')}{dR'} \right], \tag{3}$$
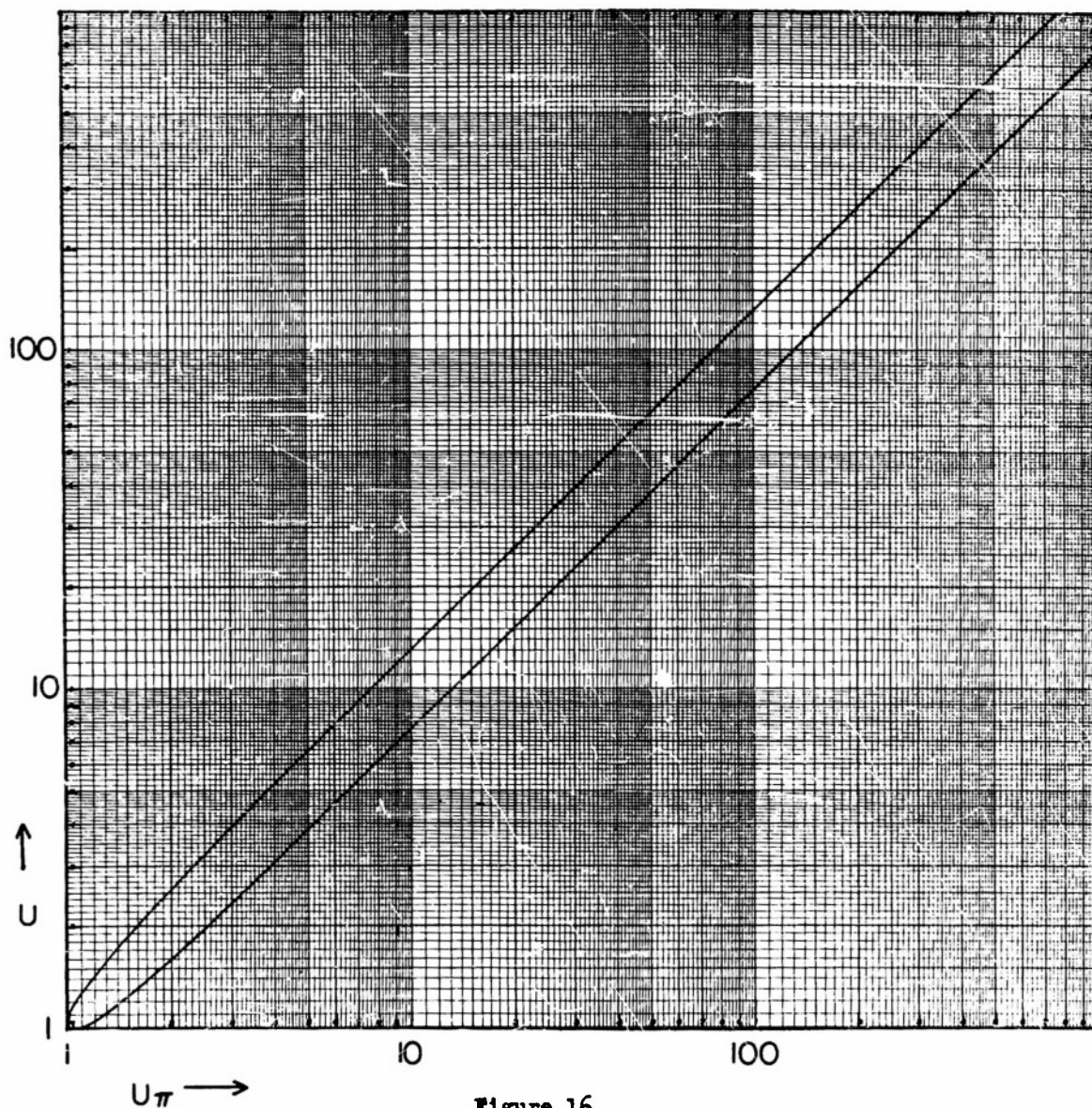
Figure 16

Energy limits of a μ-meson born from a π-meson of energy U_π. U and U_π are the total energies measured in multiples of $m_\mu c^2$ and $m_\pi c^2$, respectively.

where the residual range, R', is now to be considered as a function of U. The derivative of the collision loss, k(U), with respect to U was computed from the theoretical expression for k(U) $\left[\text{RB52, page 24, Eq. (7)} \right]$. We found by differentiation:

$$\frac{1}{k} \frac{dk}{dU} = \frac{2}{(U^2-1)U} \left[\frac{4C'}{k} \left(U^2 + \frac{1}{U^2-1} \right) - 1 \right], \tag{4}$$

where

$$C' = 0.150 \frac{m_e}{m_\mu} \frac{Z}{A}.$$

A closer inspection of Eq. (3) shows that the function $D(U)$ decreases rapidly for all energies, U, larger than a certain value so that the series given by Eq. (1) converges fairly rapidly and is, thus, convenient for the numerical evaluation of $P(U_\pi)$. We have carried out the numerical calculations concerning the energy spectrum of π-mesons at decay, $P(U_\pi)$, by making use of Eq. (IV-1), i.e., we have derived $P(U_\pi)$ not only as a function of U_π but also as a function of the geomagnetic latitude. The results are summarized in Table IV. It is evident from the previous considerations that the values of $P(U_\pi)$ corresponding to 50° geomagnetic latitude are to be looked upon as most reliable. It is, therefore, worthwhile to study the spectrum at this latitude in more detail. Fig. 17 shows the quantity $S_\pi(E)$ plotted _versus_ the kinetic energy, E, measured in Mev. This quantity is related to $P(U_\pi)$ simply by:

$$S_\pi(E) = P(U_\pi) \frac{1}{m_\pi c^2}. \tag{5}$$

The curve labeled by $S_\mu(E)$ in Fig. 17 represents the corresponding energy spectrum of μ-mesons at production. The dashed parts of the curves in the low-energy region were obtained by extrapolating Eq. (II-33) down to about 10 g cm^{-2}. It is interesting to note that the $S_\pi(E)$ displays a possible maximum at $E = 95$ Mev. Another fact which is worth mentioning is that the energy spectrum of π-mesons presented in Fig. 17 behaves in a manner very similar to that observed at high altitudes in photographic emulsions (CU50).

TABLE IV

The differential energy spectrum of π-mesons at decay (or approximately at production), $P(U_\pi)$, as a function of U_π (total π-meson energy measured in multiples of $m_\pi c^2$) for various geomagnetic latitudes, φ. The values of $P(U_\pi)$ for $U_\pi = 1.77$ were obtained by extrapolating $G(R')$ beyond $R' = 100$ g cm^{-2}, and, thus, are not a priori justified.

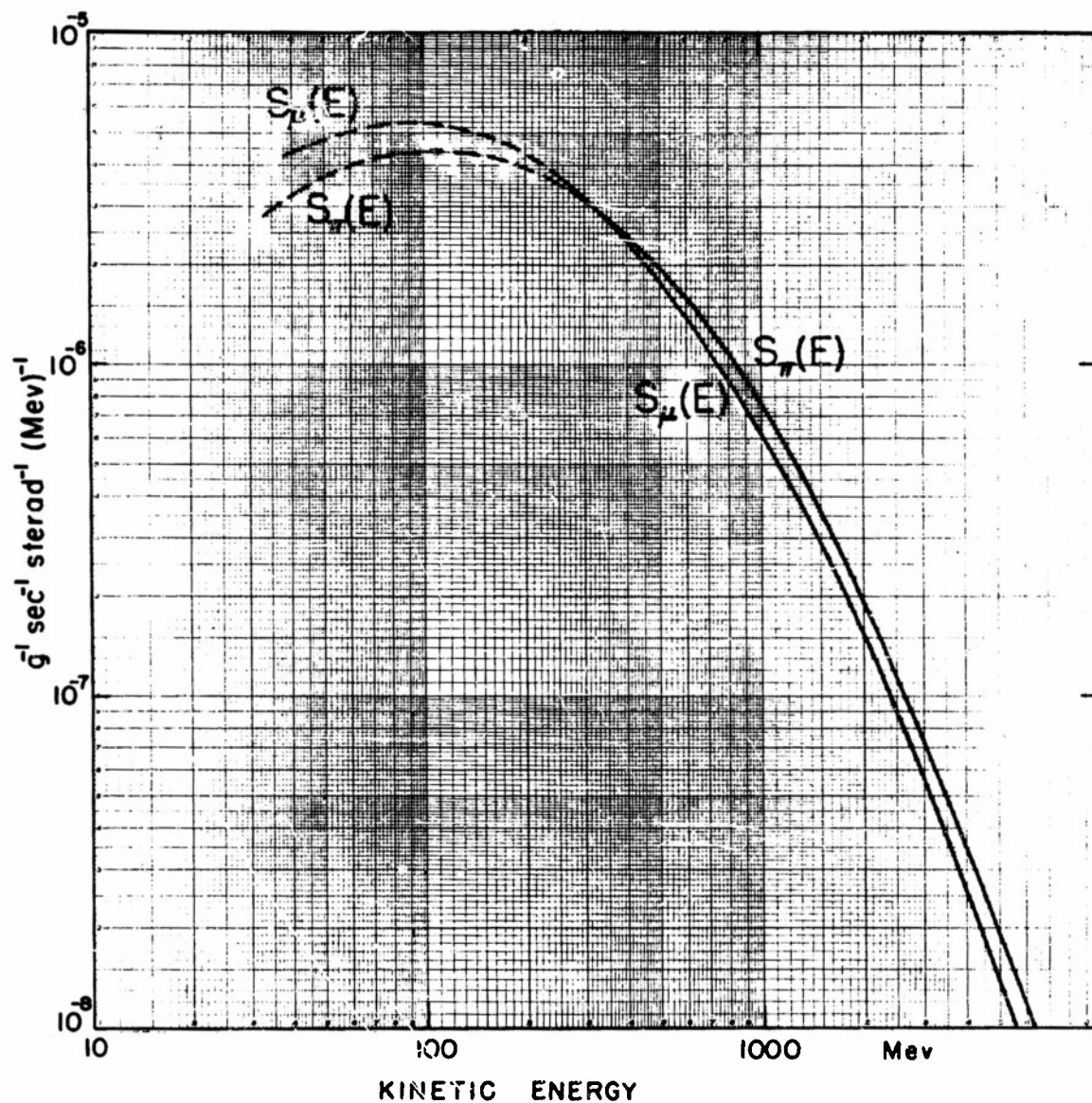| U_π	$P(U_\pi) \times 10^4$ (g^{-1}sec^{-1}sterad^{-1})					
	$\varphi = 0^\circ$	20°	30°	40°	50°	60°
1.77	(2.93)	(3.25)	(3.98)	(5.22)	(6.17)	(6.44)
2.89	2.46	2.70	3.25	4.14	4.82	5.01
4.88	1.41	1.53	1.79	2.19	2.49	2.57
8.50	0.616	0.659	0.745	0.874	0.969	0.990
14.9	0.202	0.213	0.233	0.261	0.280	0.285
26.0	0.054	0.056	0.060	0.065	0.068	0.069
45.8	0.012	0.012	0.013	0.013	0.014	0.014

Figure 17

The differential energy spectra of π-mesons and μ-mesons
at production plotted versus kinetic energy measured in Mev.
Both spectra correspond to 50° geomagnetic latitude.

C. Remarks on Multiplicity Problem.

The π-meson spectrum at decay derived in the foregoing section is almost identical to that at production; this is at least true for the energy region for which we have established the validity of Eq. (II-8). Thus, by making use of Table IV we can estimate the total number (per cm^2-sec-sterad) of π-mesons produced by the N-component at given geomagnetic latitude. Of course, since we do not know the behavior of the production spectra of π-mesons at energies smaller than a certain value E_o we are capable of computing only the following quantity:

$$\Pi(E_o) = L \int_{E_o}^{\infty} S_{\pi}(E)dE \qquad (E_o \gtrsim 260 \text{ Mev}). \qquad (6)$$

According to Eq. (6) and the definition of $S_{\pi}(E)$, $\Pi(E_o)$ represents the total number of charged π-mesons with energies greater than E_o produced in the downward cone throughout the atmosphere at given geomagnetic latitude, φ . The numerical values of $\Pi(E_o)$ for $E_o = 260$ Mev are given in the last column of Table II. By comparing this column with column 4 of Table II we note that the rate with which $\Pi(E_o)$ increases with geomagnetic latitude is much smaller than that of the integral intensity, j, of the primary radiation. This implies qualitatively that, on the average, the high-energy primaries ($E_p > 15$ Bev) produce mesons with a higher multiplicity than the primaries of energies between 2 and 15 Bev.

One can get a more quantitative idea as to the dependence of π-meson production upon the energy of the primary particle by means of the following argument:

Assume that the contribution of the secondary N-particles (neutrons, secondary protons and π-mesons) to the production of π-mesons with energies greater than E_o is negligible in comparison with that of the primary radiation. Then the quantity:

$$\bar{n}(E_o, E_p') = \frac{\Delta\Pi}{\Delta j} \qquad (7)$$

may be interpreted as the number of charged π-mesons with energies greater than E_o produced in the downward cone by one primary particle with energy

E'_p where E'_p is the effective cut-off energy of the primary flux, j, at given geomagnetic latitude. Strictly speaking, E'_p represents a properly weighted average of the cut-off energies of individual constituents of primary radiation (protons, α-particles, etc.). The quantitative data concerning the composition of primaries are as yet very wanting. However, we may assume with some certainty that most of the mesons will be produced by protons so that the values of E'_p should not depart very markedly from the cut-off energies of protons, E_p, quoted in column 2 of Table II. Thus, by identifying E'_p with E_p, we can evaluate Eq. (7) for E_o = 260 Mev as a function of E'_p if we make use of columns 7, 4 and 2 in Table II. We have estimated the values of $(\Delta \Pi / \Delta j)$ by a graphical differentiation of the curve representing Π as a function of j. The results are shown in the first column of Table V. Of course, due to the large errors involved in both Π and j, the multiplicity values quoted in Table V cannot be given much weight. (The simplifying assumptions made above reduce further the reliability of these values.) Nevertheless, we believe that our results disclose some interesting features concerning the energy dependence of the multiplicity $\bar{n}(E_o, E'_p)$. In particular, one sees that the increase of $\bar{n}$ with increasing E'_p is much more rapid at lower than at higher energies. The flattening-off begins at about 6 Bev. It is interesting to compare these results with those predicted by Fermi's statistical theory of meson production in nucleon-nucleon collisions (FE50). According to this theory, the probability to observe n π-mesons (both charged and neutral) produced in a nucleon-nucleon collision is given by:

$$f_n(w) = \frac{A}{(3n+\frac{1}{2})!} \left[\frac{251(w-2)^3}{w} \right]^n , \qquad (8)$$

where

$$w = 2\sqrt{1 + \frac{E_p}{2Mc^2}}$$

is the total energy carried by both nucleons before the collision in the center-of-mass system (w is expressed here in terms of the rest energy of the nucleon, Mc^2) and A is the normalization constant given by:

$$A^{-1} = \sum_{n=0}^{\infty} f_n(w) . \qquad (9)$$

TABLE V

Multiplicity of π-mesons produced by primaries of kinetic energies of several Bev; $\bar{n}$ is the empirical average multiplicity, i.e., the total number of π-mesons with energies greater than 260 Mev, produced throughout the atmosphere by a primary particle of energy E'_p, and emitted in the downward direction; n_t represents the theoretical multiplicity predicted by Fermi's statistical model of nucleon-nucleon collisions.

E'_p Bev	$\bar{n}$	n_t
2	0.1	0.36
4	0.5	0.66
6	1.1	0.95
8	1.3	1.03
10	1.5	1.18
12	1.6	1.30

By means of Eqs. (8) and (9) one can compute the expected average number
of charged π-mesons produced in the forward cone in the nucleon-nucleon
collision, viz.:

$$n_t \approx \frac{1}{3} \sum_{n=0}^{\infty} n f_n(w) \ . \tag{10}$$

The factor 1/3 in Eq. (10) arises from the fact that only 2/3 of all
π-mesons are charged, 1/2 of which are contained in the forward cone
of production. Using Eq. (10) we have computed the theoretical multiplicity
n_t for various primary energies of interest; the results are presented in
the second column of Table V. One sees that, at lower energies, n_t is lar-
ger by about a factor of 3-4 as compared with our empirical multiplicity,
$\bar{n}$. At higher energies (4 Bev $< E_p < 13$ Bev) the discrepancy is less pro-
nounced.

Realizing the whole crudeness with which both multiplicities, n_t and
$\bar{n}$, are derived we do not attempt to draw any definite conclusions with re-
gard to the obtained discrepancy at lower energies. However, we would
like to remark that n_t should be larger than $\bar{n}$ at lower energies due to
the fact that $\bar{n}$ contains only π-mesons with energies greater than $E_0 = 260$ Mev.
Furthermore, it is likely that Fermi's multiplicity will be reduced at
lower energies if one takes into account the plural processes which occur
inside the air nucleus during the nucleon-nucleon collision. Such a re-
duction is expected, for instance, from a simple model of the air nucleus
suggested recently by U. Haber-Schaim (HS51). Finally, the empirical
average multiplicity contains contributions of π-mesons stemming from the
second, third and higher generations. These contributions can be considered
as negligible only at lowest energies of primary particles; at primary ener-
gies greater than 10 Bev they become as important as those stemming from the
first generation.

APPENDIX

Consider the following definite integral:

$$F(a,b) = \int_a^b g(z)f(z)dz , \qquad (A-1)$$

where $g(z)$ and $f(z)$ are bounded functions in the closed interval (a,b). According to the mean-value theorem of integral calculus one may write for $F(a,b)$ also:

$$F(a,b) = g(\xi) \int_a^b f(z)dz , \qquad (A-1')$$

where ξ is a specific value of z lying somewhere between a and b. In general the value of ξ is not better known. However, in some special cases one can estimate the value of ξ fairly accurately. This is so, for example, if the function $g(z)$ and $f(z)$ satisfy the following conditions, respectively:

(1) $g(z)$ is a slowly varying analytical function in the closed interval (a,b):

(2) $f(z)$ displays a single sharp maximum in the closed interval (a,b).

In this case it is convenient to expand the function $g(z)$ in the integrand of Eq. (A-1) into Taylor's series at the point ξ', determined by the following equation:

$$\xi' \int_a^b f(z(dz = \int_a^b zf(z)dz . \qquad (A-2)$$

At this point Eq. (A-1) becomes:

$$F(a,b) = \int_a^b \left[g(\xi') + \frac{1}{2}(z-\xi')^2 g''(\xi') + \dots \right] f(z)dz . \quad (A-3)$$

Now, owing to condition (1), one may neglect to a good approximation the terms involving the derivatives higher than the first. By doing so and by setting $\xi' = \xi$ one sees that Eq. (A-3) becomes identical to Eq. (A-1').

The relative error which one makes by neglecting higher derivatives of $g(z)$ is of the order of magnitude of

$$\text{relative error} = \frac{1}{2} \frac{g''(\xi)}{g(\xi)} \left[\sigma^2 - \xi^2 \right] \quad , \qquad (A-4)$$

where

$$\sigma^2 \int_a^b f(z)dz = \int_a^b z^2 f(z)dz \ .$$

Owing to condition (2) the value of σ will not differ markedly from that of ξ . Thus, the relative error can be reduced considerably if the two conditions above are well satisfied.

ACKNOWLEDGMENTS

BIBLIOGRAPHY

(AG50)   G. Ascoli;   Phys. Rev. 79, 812 (1950).

(BPM38)   P.M.S. Blackett;   Phys. Rev. 54, 973 (1938).

(BRH49)   Brown, Camerini, Fowler, Heitler, King and Powell;
                                      Phil. Mag. 40, 862 (1949).

(CDE50)   D.E. Caro, J.K. Parry, H.D. Rathgeber;
                                      Aust. J. Sci., Res. A, 4, 16 (1950).

(CM50)   M. Conversi;   Phys. Rev. 79, 750 (1950).

(CU50)   U. Camerini, P.H. Fowler, W.O. Lock, H. Muirhead;
                                      Phil. Mag. 41, 413 (1950).

(DA44)   A. Duperier;   Terr. Magn. Atmos. Elect. 49, 1 (1944).

(DA48)   A. Duperier;   Proc. Phys. Soc. 61, 34 (1948).

(DA49)   A. Duperier;   Proc. Phys. Soc. 62, 684 (1949).

(DEW51)   D.W.N. Dolbear, H. Elliot;
                                      J. Atmos. Terr. Phys. 1, 215 (1951).

(FE50)   E. Fermi;   Prog. Theor. Phys. 5, 570 (1950).

(HB44)   B. Haurwitz, J.M. Austin;
                                      Climatology, McGraw-Hill Book Co.,
                                      New York and London (1944).

(HS51)   U. Haber-Schaim;   Phys. Rev. 84, 1199 (1951).

(KW49)   W.L. Kraushaar;   Phys. Rev. 76, 1945 (1949).

(NHV52)   H.V. Neher;   Chapter V, Progress in Cosmic-Ray Physics,
                                      North-Holland Publishing Co., Amster-
                                      dam (1952).

(RB47)   Rossi, Sands, and Sard;   Phys. Rev. 72, 120 (1947).

(RB48)   B. Rossi;   Rev. Mod. Phys. 20, 543 (1948).

(RB52)   B. Rossi;   High-Energy Particles, Prentice-Hall Pub-
                                      lishing Co., New York (1952).

(RL52)   L. del Rosario, J. Dávila-Aponte;
                                      Technical Report No. 1, Department of
                                      Physics, University of Puerto Rico,
                                      (1952).

(SM49)   M. Sands;   Technical Report No. 28, LNSE, Massa-
                                 chusetts Institute of Technology, (1949).

(TJH48) J.H. Tinlot;   Phys. Rev. 73, 1476 (1948); 74, 1197
                                 (1948).

(WJR50) J.R. Winckler, T. Stix, K. Dwight, R. Sabin;
                                 Phys. Rev. 79, 656 (1950).